

Article

Mineral Chemistry of Olivine, Oxy-Spinel, and Clinopyroxene in Lavas and Xenoliths from the Canary, Azores, and Cape Verde Islands (Macaronesia, North Atlantic Ocean): New Data and Comparisons with the Literature

Federica Zaccarini ^{1,*}, Giorgio Garuti ¹, Reinhard Moser ², Constantinos Mavrogonatos ³, Panagiotis Voudouris ³, Adriano Pimentel ⁴ and Sabrina Nazzareni ⁵

Citation: Zaccarini, F.; Garuti, G.; Moser, R.; Mavrogonatos, C.; Voudouris, P.; Pimentel, A.; Nazzareni, S. Mineral Chemistry of Olivine, Oxy-Spinel, and Clinopyroxene in Lavas and Xenoliths from the Canary, Azores, and Cape Verde Islands (Macaronesia, North Atlantic Ocean): New Data and Comparisons with the Literature. *Minerals* **2024**, *14*, 161. <https://doi.org/10.3390/min14020161>

Academic Editor: Alexandre V. Andronikov

Received: 8 December 2023

Revised: 17 January 2024

Accepted: 30 January 2024

Published: 1 February 2024



Copyright: © 2024 by the authors. Licensee MDPI, Basel, Switzerland. This article is an open access article distributed under the terms and conditions of the Creative Commons Attribution (CC BY) license (<https://creativecommons.org/licenses/by/4.0/>).

¹ Geosciences Programme, Faculty of Science, University Brunei Darussalam, Jalan Tungku Link, Gadong, Bandar Seri Begawan BE1410, Brunei; giorgio.garuti1945@gmail.com

² Department of Pediatrics and Adolescent Medicine, Landeskrankenhaus LKH Hochsteiermark, 8700 Leoben, Austria; reinhard.moser@kages.at

³ Faculty of Geology and Geoenvironment, National and Kapodistrian University of Athens, 15784 Athens, Greece; kmavrogon@geol.uoa.gr (C.M.); voudouris@geol.uoa.gr (P.V.)

⁴ Instituto de Investigação em Vulcanologia e Avaliação de Riscos (IVAR), Universidade dos Açores, 9500-321 Ponta Delgada, Portugal; adriano.hg.pimentel@azores.gov.pt

⁵ Dipartimento di Scienze Chimiche, della Vita e della Sostenibilità Ambientale, Università di Parma, 43124 Parma, Italy; sabrina.nazzareni@unipr.it

* Correspondence: federicazaccarinigaruti@gmail.com; Tel.: +43-664-3868590

Abstract: An electron microprobe study was carried out on olivine, clinopyroxene, and oxy-spinel occurring in basalts and dunite xenoliths from the archipelagos of the Azores, the Canary Islands, and Cape Verde. By comparing our results with previously published data from the volcanic islands of Macaronesia, we confirmed the validity of the compositions of olivine, clinopyroxene, and oxy-spinel as geochemical tracers. The origin of olivine, i.e., crystallized in the lithospheric mantle or in volcanic rocks, was successfully discriminated. Olivine from Lanzarote dunite xenoliths, which represent fragments of the mantle transported to the surface by host magmas, exhibited higher Fo% values (Fo_{91.02} to Fo_{91.94}) and a different distribution of minor elements Ca, Ni, and Mn (CaO up to 0.42 wt%, NiO 0.07–0.41 wt%, MnO 0.06–0.3 wt%) when compared with olivine occurring as phenocrysts in basaltic lavas from the Macaronesian islands. The highly variable forsterite contents (Fo_{75.1} to Fo_{94.4}) in olivine from gabbro and peridotite xenoliths found across the islands of Macaronesia were attributed to fractional crystallization that started in a deep magma reservoir, suggesting that these xenoliths represent cumulate rocks and not mantle fragments. Alternatively, these xenoliths may have been affected by the interaction with metasomatic fluids. The composition of clinopyroxene phenocrysts was used to decipher formation conditions under extensional tectonics. Their composition suggests that the host lavas have an alkaline to calc-alkaline signature. Furthermore, clinopyroxene euhedral shapes and compositions suggest an origin by fractional crystallization in a closed magmatic system. The composition alone of oxy-spinel from Macaronesian basalts and xenoliths was not sufficient to draw conclusions about the geodynamic environment where they were formed. Nevertheless, the relationship between oxy-spinel and olivine crystallized in equilibrium was successfully used as oxybarometers and geothermometers. The oxy-spinel–olivine pairs show evidence that the basaltic lavas were crystallized from melts with higher oxygen fugacity and different cooling histories than those of the mantle xenoliths, as the latter crystallized and re-equilibrated much slower than the basalts.

Keywords: olivine; clinopyroxene; oxy-spinel; electron probe microanalyses; lavas; xenoliths; Macaronesia archipelagos

1. Introduction

Since the establishment of the Plate Tectonics theory, numerous contributions have been published focusing on mantle processes using a wide variety of study methods. Undoubtedly, mineralogical and geochemical studies still hold the privilege of revealing the most critical information, especially in terms of mantle composition, evolution in space and time, and geodynamics [1–4].

Olivine, oxy-spinel, and clinopyroxene are major mineralogical components of the upper mantle and a variety of mafic–ultramafic igneous rocks such as peridotite, gabbro, and basalts. Olivine, oxy-spinel, and pyroxene are often the early crystallized phases in magmatic systems, and their crystal structures are able to record different processes involved during the evolution of the host rocks. Their mineral chemistries have long been recognized as a reflection of the parental melt composition and crystallization conditions in terms of temperature, pressure, and oxygen fugacity. Olivine and pyroxene, for example, can incorporate various amounts of trace elements, and the related diffusion processes can be used to reconstruct and/or estimate timescales of events in volcanic systems (see [1] and references therein). Therefore, these minerals have become powerful petrogenetic indicators for deciphering the origin of terrestrial magmas and the geodynamic setting of their mantle sources [2–32].

Among other mantle-related features on our planet, the case of ocean island volcanoes remains poorly understood. Their complexities in terms of their geodynamic setting, i.e., intraplate versus near mid-ocean ridge settings, magma composition, and eruptive behavior, have attracted a broad scientific audience that struggles to unravel the evolutionary history of these island volcanoes. Prominent examples of ocean island volcanoes are found in Hawaii, the Galápagos, the Azores, Madeira, Cape Verde, and the Canary Islands [33].

This contribution provides electron probe microanalyses of olivine, clinopyroxene, and chromium oxy-spinel from volcanic rocks and xenoliths ejected in volcanic rocks of Macaronesia archipelagos (Azores, Canaries, and Cape Verde), which are located in the central-eastern North Atlantic Ocean (Figure 1A–D). The Macaronesian islands were built by submarine volcanism that evolved into subaerial activity and are all related to mantle plumes intersecting the North Atlantic oceanic crust [34,35]. Macaronesia is a group of archipelagos with a complex and interesting volcanological history that is far from being fully understood.

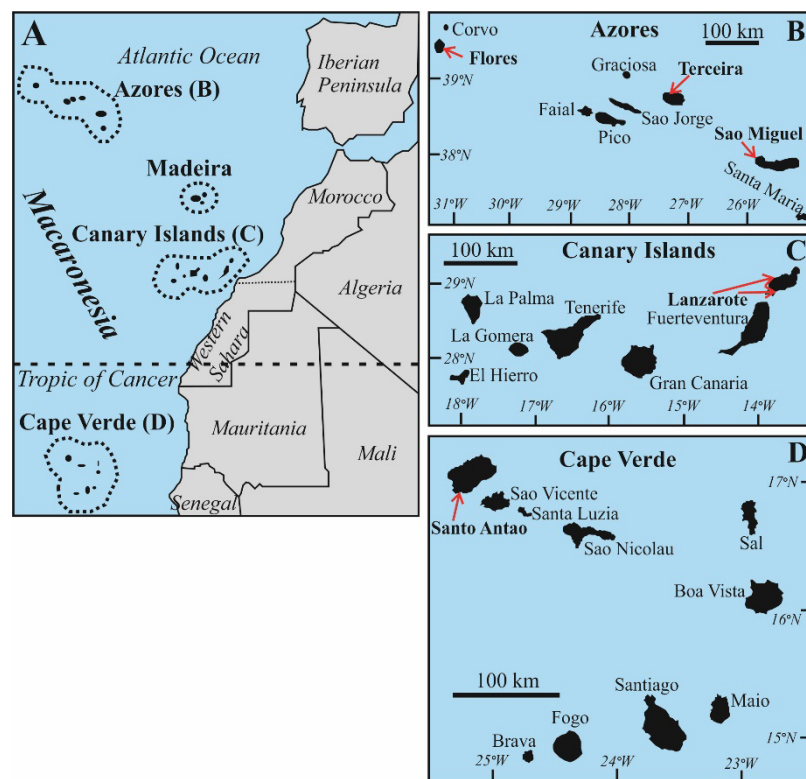


Figure 1. Geographical location of Macaronesia (A), Azores (B), Canary Islands (C), and Cape Verde (D) archipelagos. The red arrows show the location of the studied samples.

The comparison of the mineralogical results obtained in this study with those previously published on the Macaronesian islands provides further elements for the discussion of some aspects related to the origin, evolution, and crystallization conditions of the volcanic rocks and associated xenoliths. We also confirm the validity of the composition of olivine, clinopyroxene, and oxy-spinel as geochemical tracers.

2. Provenance of the Studied Samples and Source of Literature Data

The provenance and a brief description of the samples analyzed in this study (Figure 1A–D) are listed in Table 1, and the literature data are summarized in Table S1. The samples include different types of lavas and mafic–ultramafic xenoliths (gabbro, wehrlite, dunite, clinopyroxenite, harzburgite, and lherzolite) from the Macaronesian archipelagos of Azores, Cape Verde, the Canary Islands, and Madeira.

Table 1. Description of the samples from Macaronesia analyzed in this work. (listed from north to south).

Island	Location	Type of Rock	Geographic Coordinates
Azores:			
Flores	Lagoa Funda	Basalt tuff	39°39'82" N, 31°21'49" W
Terceira	Pico Gordo	Basalt flow	38°80'02" N, 27°26'20" W
Sao Miguel	Sete Cidades	Lava flow	37°53'56" N, 25°49'17" W
Canary Islands:			
Lanzarote	Playa Malva	Dunite xenolith, basalt	29°03'50" N, 13°46'03" W
	Puerto Calero	Dunite xenolith, basalt	28°54'59" N, 13°42'28" W
Cape Verde:			
Santo Antao	Tarrafal	Nephelinite–phonolite series	16°57'17" N, 25°18'29" W

2.1. Geological Setting and Sample Selection from the Macaronesia Archipelagos

2.1.1. Azores Islands

The Azores archipelago is located in the North Atlantic Ocean at the triple junction of the North American, Eurasian, and African lithospheric plates, approximately 1400 km west of the Iberian Peninsula and between 37° and 40° Lat. N and 25–31° Long. W (Figure 1A,B). The archipelago consists of nine islands, straddling the Mid-Atlantic Ridge (MAR), which are geographically divided into three groups: (1) the Western Group formed by Flores and Corvo islands lying west of the MAR in the North American plate, (2) the Central Group constituted by Graciosa, Terceira, São Jorge, Pico, and Faial, and (3) the Eastern Group formed by São Miguel and Santa Maria. The islands of the Central and Eastern groups lie east of the MAR, astride the diffuse boundary of the Eurasian and African plates [36–38].

The oldest island of the Azores is Santa Maria, with an age of 6.01 Ma [39], and Pico is the youngest, with an age of 0.27 Ma [40], thus being among the youngest islands of Macaronesia. Volcanism in the Azores is generally accepted as a result of the complex interaction between a mantle melting anomaly, often referred to as the Azores mantle plume, and the plate triple junction [41–43]. Seven of the nine islands have active volcanic systems (fissure zones and central volcanoes), a number of which have erupted in historical times (i.e., in the last 500 years). The subaerial volcanic rocks of the Azores are predominantly mafic (basalts, alkali basalts, and hawaiites), along with subordinate felsic compositions from trachytes to pantellerites [44].

The samples studied in this work were collected from the islands of Flores, Terceira, and São Miguel (Figure 1B and Table 1). The sample from Flores (AZMO2) consists of a Late-Holocene basaltic tuff from the Lagoa Funda hydromagmatic deposit [45], located in the middle of the island (Figure 1B). The sample from Terceira (AZMO1) comes from the Pico Gordo basaltic lava flow (see [46]) of the Mid-Holocene age, collected from the sea cliff on the north of the island. Samples AZMO3 and AZPG6 from São Miguel were collected in the Mosteiros lava delta outcrop in the western part of the island, at 37°53'56".

2.1.2. The Canary Islands

The Canary Islands geologically pertain to the Atlantic zone of the African plate, located about 100–500 km west of the Sahara coast, at 28°–29° Lat N and 13°–18° Long W. (Figure 1C). From east to west, the main islands are Lanzarote, Fuerteventura, Gran Canaria, Tenerife, La Gomera, La Palma, and El Hierro. Several volcanic rock types have been described in the Canary Islands, including alkali basalts, basanites, phonolites, trachytes, nephelinites, trachyandesites, tephrites, and rhyolites [34,35].

Due to their proximity to the northwest coast of Africa (Figure 1C), two volcanological models have been proposed: (1) magmatism related to the presence of regional crustal fractures extending from the Atlas Mountains of Morocco to the ocean; (2) magmatism driven by the slow movement of the African plate over a mantle plume. Currently, the mantle plume model is more widely accepted for the Canary Islands's magmatism [47,48].

Geochronological data obtained on the oldest sub-aerially-erupted lava demonstrated a decrease in the age of the island formation from east to west along the archipelago: Lanzarote (>15 Ma), Fuerteventura (24 Ma), Gran Canaria (15 Ma), Tenerife (12 Ma), La Gomera (12 Ma), La Palma (2 Ma,) and El Hierro (1 Ma) [17,35]. In the past, the islands of Lanzarote and Fuerteventura constituted a single volcanic edifice [34,35].

The samples collected in Lanzarote (Figure 1C and Table 1) consist of basaltic olivine-rich lavas. They were sampled in the outcrops of Playa Malva (samples LZ2019) and Puerto Calero (sample LZ1), located in the N-W and S-W sectors of the island, respectively. Samples from Playa Malva are Pleistocene–Holocene basalts (IGME web site <https://igme.maps.arcgis.com/apps/mapviewer/index.html>, accessed on 17 January 2024) containing a great number of xenoliths with variable sizes, from 1 to 15 cm. Due to its easy accessibility and abundance around Puerto Calero, the basalt hosting the xenoliths is widely used as a building stone.

2.1.3. The Cape Verde Islands

The archipelago of Cape Verde consists of a main group of islands, namely, from east to west, Boa Vista, Sal, Maio, Santiago, Sao Nicolao, Fogo, Brava, Santa Luzia, Sao Vicente, and Santo Antao (Figure 1D). They are located in the North Atlantic Ocean about 600–900 km west of Mauritania and Senegal, approximately between 15–17° Lat N and 23–25° Long W (Figure 1D). There is a general consensus that the Cape Verde archipelago is a classical hotspot underlain by an active mantle plume. The volcanism has a highly alkaline affinity, as evidenced by the presence of feldspathoids. Most of the Cape Verde lava compositions vary from basanite to mela-nephelinite and textures from aphyric and olivine-clinopyroxene porphyritic. Similar to the Canary Islands, there is a general decrease in the age from east to west. In particular, Boa Vista, Sal, and Maio are older than 20 Ma, Santiago and Sao Nicolao are 11 and 10 Ma, respectively, whereas the other islands have an age ranging between approximately 6 and 7 Ma [35]. The investigated samples (CV1–4) were collected close to Tarrafal in the west of Santo Antao Island (Figure 1D and Table 1). The oldest exposed rocks in the area have an age of about 7.6 Ma [47], although the studied samples belong to the so-called young Tarrafal group, which is about 0.4–0.2 Ma old [20].

2.2. Selected Data from Literature

In order to provide a statistically significant amount of data for the archipelagos of Macaronesia, we have compared our mineralogical results with those available in the literature (Table S1). In particular, published data on mafic minerals concern

- (1) The Azores Islands; lavas and xenoliths of Corvo and Sao Miguel islands [14,28–32];
- (2) The Canary Islands; different types of lavas from Gran Canaria, El Hierro, La Gomera, Lanzarote, La Palma, and Tenerife [8,9,11,13,15–17,19], and various xenoliths from Fuerteventura, Hierro, Lanzarote, La Palma, and Tenerife [5,10,18,22,24,26,49];
- (3) Cape Verde; lavas from Santo Antao and Santiago islands [12,20] and xenoliths from Sal [21];
- (4) Madeira; olivine and oxy-spinels hosted in the lava [13,23].

3. Analytical Techniques

Several thin sections from each sample were previously studied by a transmitted-light microscope (Olympus, Tokyo, Japan). Electron probe microanalyses were carried out at the Eugen F. Stumpfl Laboratory of the Leoben University, Austria, with a Superprobe Jeol JXA 8200 using both energy dispersive (EDS) and wavelength dispersive (WDS) systems. Back-scattered electron (BSE) images were obtained using the same instrument using both EDS and WDS systems. Back-scattered electron (BSE) images and elemental distribution maps were obtained using the same instrument. Quantitative analyses of olivine, pyroxene, and spinel were performed using an accelerating voltage of 20 kV, an electron beam current of 50 nA, and a beam diameter of about one micrometer. Corrections for inter-elemental effects were made using a ZAF procedure that takes into account the (1) atomic number, which affects the penetration of incident electrons into the material, (2) absorption of X-rays in the specimen, and (3) fluorescence effect caused by other X-rays generated in the specimen. The analyses of Na, Mg, K, Al, Si, Ca, Ti, V, Cr, Zn, Mn, P, Fe, Co, and Ni were obtained using the $K\alpha$ lines and were calibrated using kaersutite, sphalerite, and synthetic metallic vanadium. The following analyzing crystals were selected: TAP for Na, Mg, and Al; PETJ for K, Si, Ca, and P; LIFH for Ti, V, Cr, Zn, Mn, Fe, Co, and Ni. The peak and background counting times were 20 and 10 s, respectively, for the major elements. They were increased to 120 and 60 s for the trace elements in order to decrease the detection limits. The detection limits were automatically calculated by the Jeol microprobe software, and they are listed as follows (in ppm): Ca (50), Na, Mg, K, Fe, Mn, P (100), Al, V, Ni, Co (150), Cr, Zn (200), Si, and Ti (250). The amount of Fe^{3+} in oxy-spinel was calculated by assuming the ideal spinel stoichiometry. Despite the low detection limits achieved using the selected conditions, based on the analytical precision (reproducibility

and repeatability), reliable values of the trace elements in olivine were obtained for Mn, Ni, and Ca, and thus, only these elements are discussed further in this work. The same instrument was used to obtain back-scattered electron images (BSE) and X-ray elemental distribution maps. The compositions of olivine, clinopyroxene, and oxy-spinel are available in Tables S2–S4.

4. Results of the Present Work and Comparison with Literature

4.1. Texture and Composition of Olivine

Macroscopic characters and field relations of the samples investigated are exemplified in Figures 2A–C and 3A–F.



Figure 2. Examples of the collected hand samples. Lava containing several crystals of olivine, up to about 1 cm in size, in the sample from Azores (A) and from Cape Verde (B). Xenolith from Lanzarote (C).

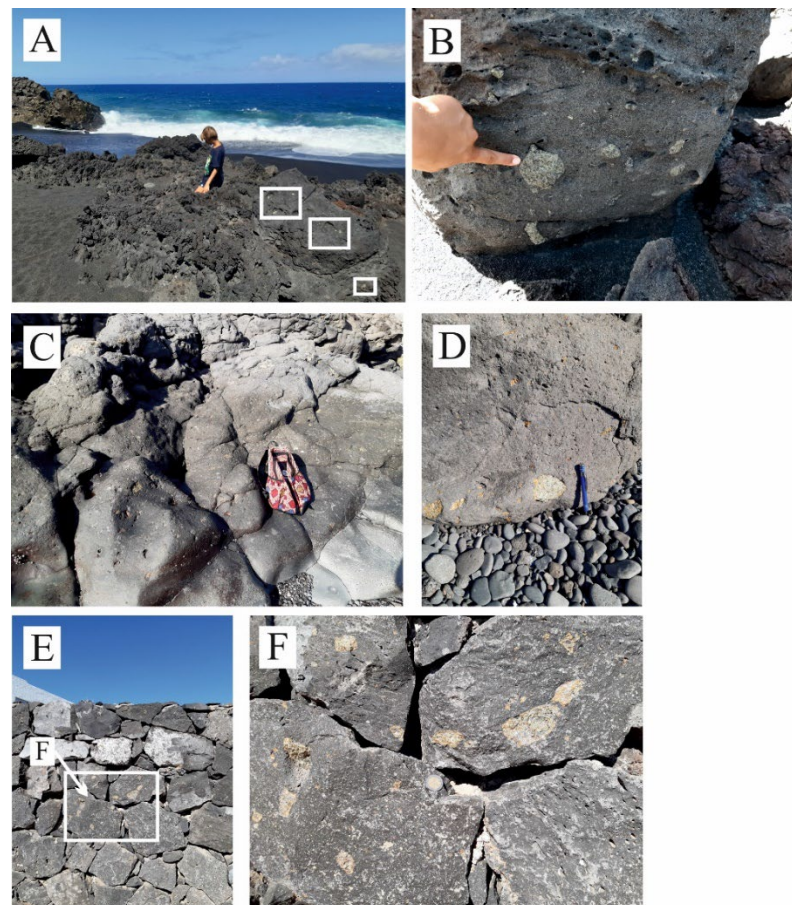


Figure 3. General overview of selected xenoliths from Lanzarote: (A) outcrop of Playa Malva (the white squares point the area enriched in xenoliths), (B) detailed view of the basalt containing the

xenoliths in Playa Malva, (C) outcrop of Puerto Calero, (D) large xenoliths in the Puerto Calero lava, (E) wall built of basalt enriched in xenoliths in Puerto Calero, (F) detail of the wall.

In the lavas from Flores, Terceira, São Miguel (Azores), Lanzarote (Canaries), and Santo Antao (Cape Verde), olivine occurs as crystals up to 1 cm in size, disseminated throughout the lava groundmass (Figure 2A,B). In contrast, olivine forms about 90% by volume in the xenoliths from Lanzarote, consistent with a dunite mineral assemblage. The xenoliths may vary in size from 1–2 cm, up to 10 cm or more and generally occur as isolated nodules chaotically distributed in the lava (Figure 3F). However, peridotite xenoliths arranged in dense clusters have been locally observed in the basalt of Playa Malva (Figure 3A,B) and Puerto Calero (Figure 3D–F).

Under the optical microscope, olivine in the lavas generally occurs as euhedral phenocrysts or sometimes as resorbed grains (Figure 4A–E). In the xenoliths, large olivine crystals are arranged in a massive texture (Figure 4F–H) along with minor clinopyroxene, oxy-spinel, and rare orthopyroxene. The contacts between the xenolith and the host lava are always sharp (Figure 4F,G) and are locally marked by weak serpentine alterations of olivine along the grain boundaries and cracks, which are sometimes filled with a glassy material (Figure 4F–H).

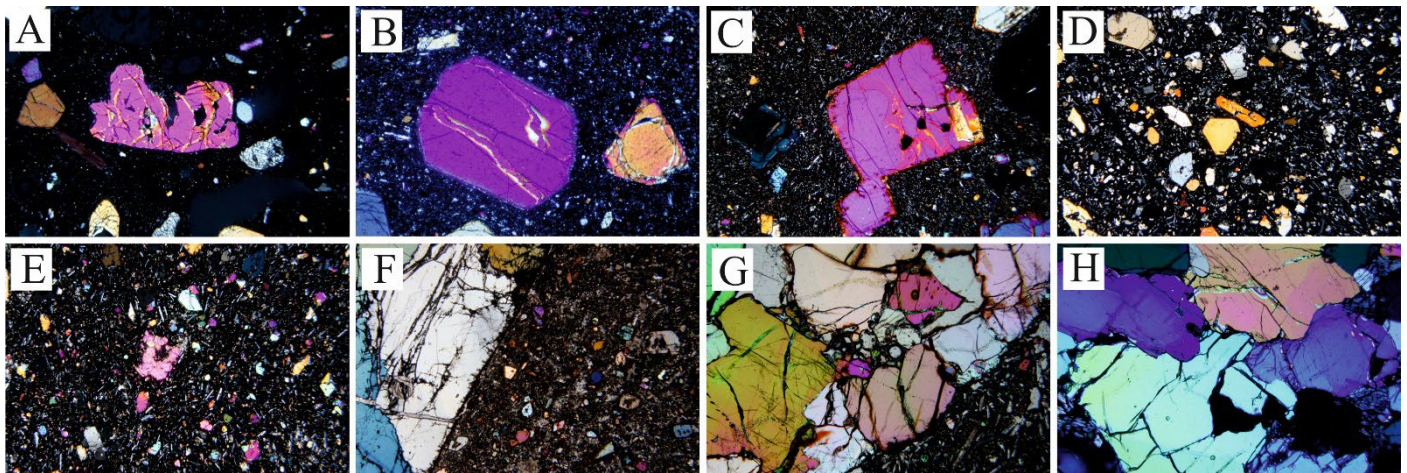


Figure 4. Cross-polarized transmitted light photomicrographs of thin sections showing various modes of olivine occurrence: (A) large and irregularly shaped crystal of olivine in the basalt of Sao Miguel, Azores, (B) large euhedral olivine in the basalt of Sao Miguel, Azores, (C) large olivine in the basalt of Santo Antao, Cape Verde, (D) variably sized olivine crystals in the basalt of Santo Antao, Cape Verde, (E) crystals of olivine in the lava of Playa Malva, Lanzarote, (F) contact between large crystal of olivine in the xenolith and the host lava from Playa Malva, Lanzarote, (G) contact between large crystal of olivine in the xenolith and the host lava from Puerto Calero, Lanzarote, (H) olivine in the xenolith from Puerto Calero, Lanzarote. The width of the pictures is 4 mm.

In general, olivine crystals from both host lavas and xenoliths appear homogenous in composition or display thin rims of a few micrometers, enriched in Fe, as is visible in the X-ray element-distribution maps (Figure 5A,B). Major variations concern the Mg/Fe ratio expressed as a forsterite number [$\text{Fo}\% = \text{Mg}/(\text{Mg} + \text{Fe}) \times 100$] and the concentration of trace elements (Ca, Mn, Ni) as a function of the forsterite number. Variations in chemical parameters in our samples (Figure 6A–C) clearly show two distinct groups of olivine compositions. One group is characterized by a narrow range of the Fo% from 90.58 to 91.75, high NiO (0.25–0.43 wt%), low MnO (0.06–0.18 wt%), and Ca (<1000 ppm) concentrations. It mainly consists of olivine from the xenoliths of Lanzarote, along with a few analyses of accessory olivine from the host basalt (Figure 6A–C). The second group comprises olivine phenocrysts from the lavas of Lanzarote (Canary Island), Azores, and Cape Verde. These olivine crystals are characterized by a wide variation in forsterite content (Fo% = 71.27–89.70), low NiO (0.04–0.28 wt%), high MnO (0.12–0.35 wt%), and Ca (700–5500 ppm) concentrations.

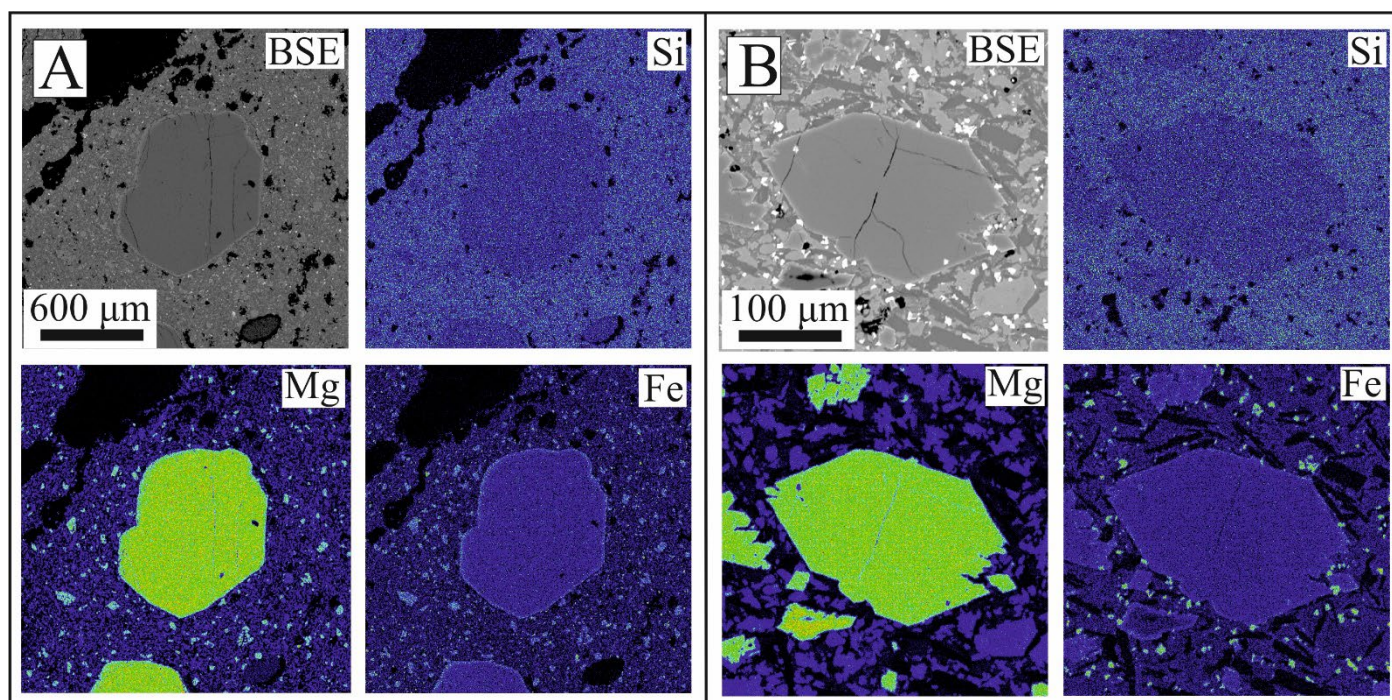


Figure 5. Back-scattered electron (BSE) image and X-ray element-distribution maps of Si, Mg and Fe in olivine from Terceira basalt, Azores (A) and from Playa Malva xenolith, Lanzarote (B). Warm colors (yellow to red) denote high concentrations, cold colors (green to violet), low concentrations.

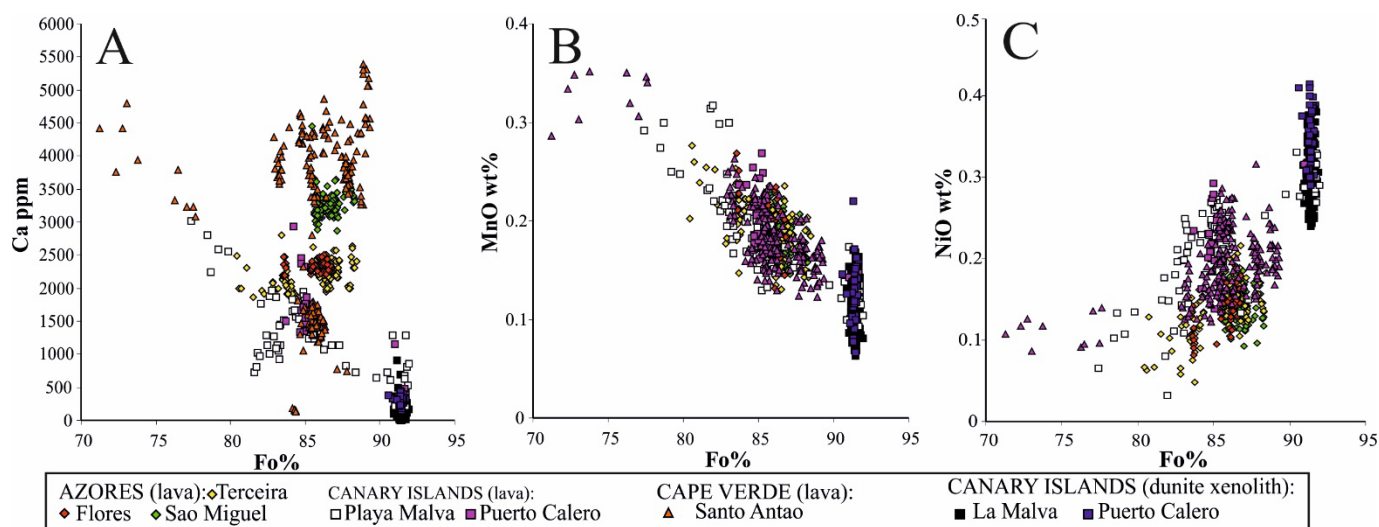


Figure 6. Compositional variation in Ca (ppm) (A), MnO (wt%) (B), and NiO (wt%) (C) as a function of forsterite molar % in the olivine from the samples analyzed in this contribution.

Co-variation diagrams show that Mn and Ca are negatively correlated with Fo% (Figure 6A,B), which is in contrast with Ni, which tends to have a positive correlation (Figure 6C).

A comparison with literature data (Figure 7A–C) shows that olivine from the lavas display variation trends of Ca, Mn, and Ni similar to our samples (Figure 6A–C), although they have a wider range of forsterites, varying from about 90 to less than 60 Fo%. The lowest values have been recorded in some analyses from Corvo and Sao Miguel (Azores), and La Gomera (Canary Islands) is characterized by Fo < 70% and extremely low values of NiO (<0.1 wt%) but high concentrations of MnO (0.6–1.13 wt%).

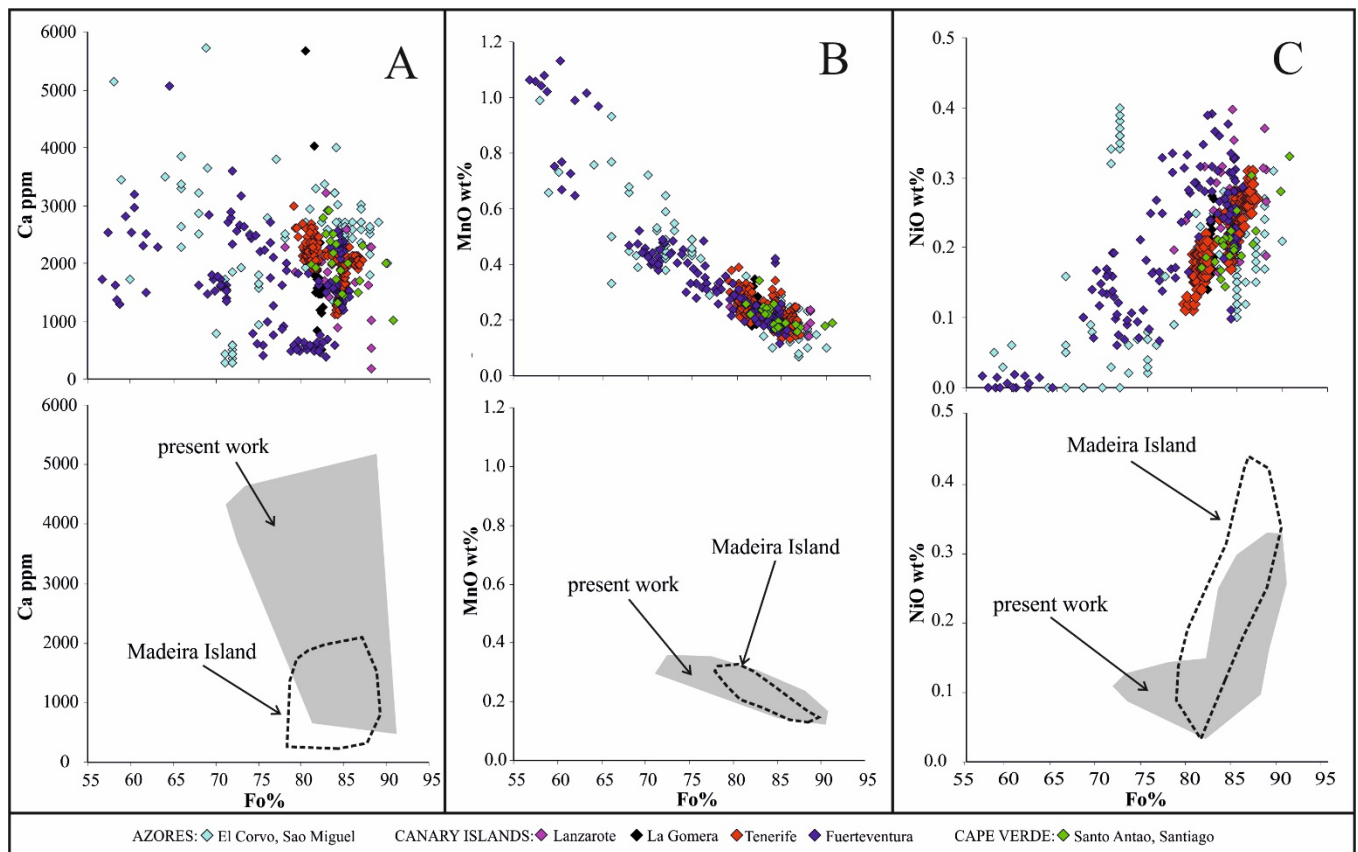


Figure 7. Compositional variation in Ca (ppm) (A), MnO (wt%) (B) and NiO (wt%) (C) as a function of forsterite molar % in the olivine from lavas (literature data, see Table S1 for references) and comparison with present work. Compositional fields were drawn because more than 300 analyses were available.

Literature data for xenolith olivine display a variation in the forsterite content between 43.8 and 94.4 Fo%, although most of the analysis plots are in the range of 78–92 Fo% (Figure 8A–I). Values higher than 90 Fo%, similar to dunite xenoliths analyzed in this work, have been found in peridotite xenoliths (Iherzolite, harzburgite, dunite) from Santa Maria (Azores), Sal (Cape Verde), El Hierro, La Palma, Fuerteventura, and Lanzarote (Canaries). The lowest values (<70 Fo%) have been detected in gabbro xenoliths from Corvo (Azores), Tenerife, La Palma, and Lanzarote (Canary Islands). Few xenoliths with wehr-lite-type mineralogy that have an intermediate forsterite number between 80–85 Fo% have been detected in La Palma.

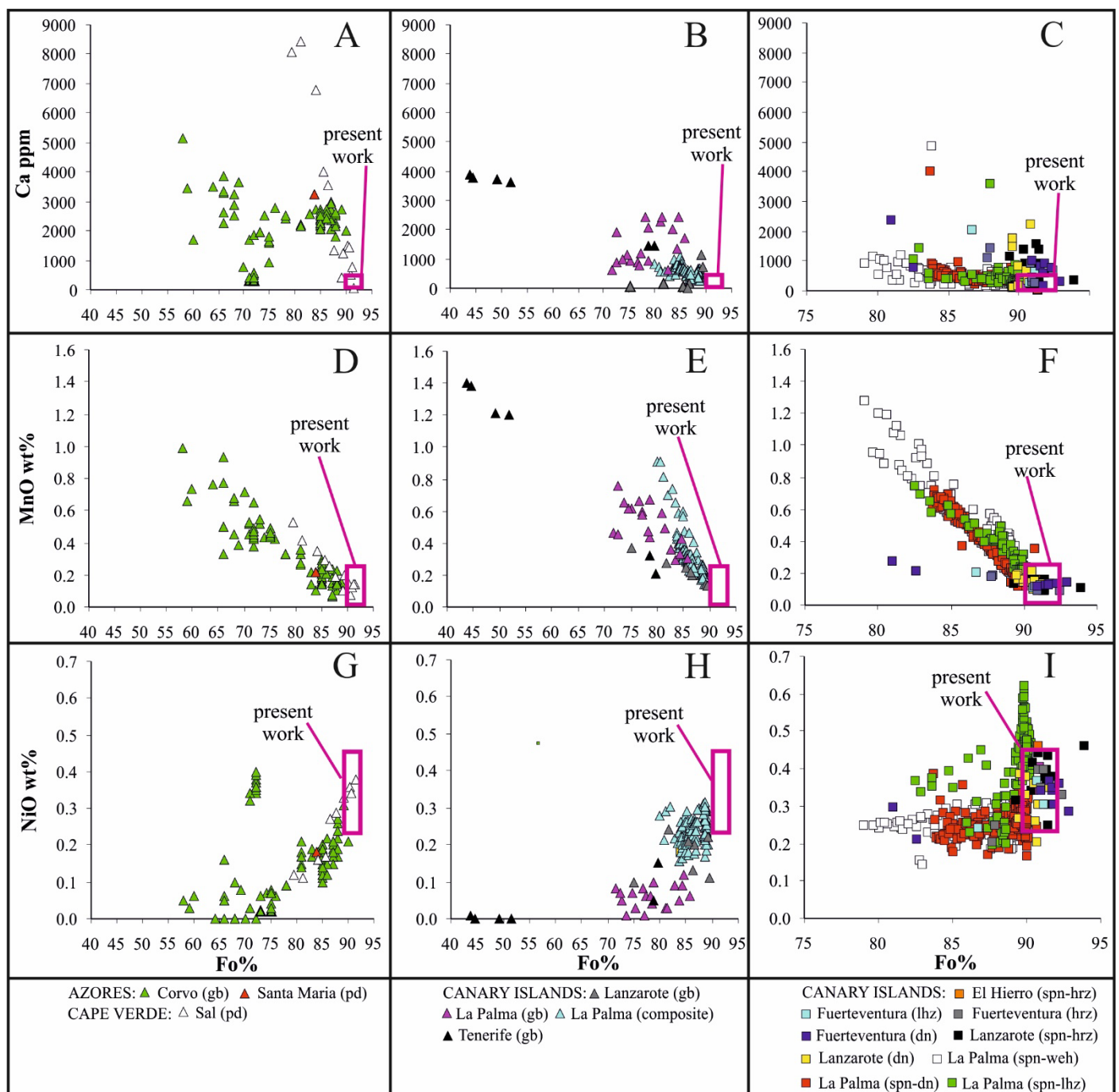


Figure 8. Compositional variation in Ca (ppm) (A–C), MnO (wt%) (D–F) and NiO (wt%) (G–I) as a function of forsterite molar % in the olivine from xenoliths. Abbreviation: gb = gabbro, pd = peridotite, spn-lhy = spinel lherzolite, lhz = lherzolite, hrz = harzburgite, dn = dunite, spn-hrz = spinel harzburgite, spn-weh = sinel wehrlite, spn-dn = spinel dunite. Literature data (see Table S1 for references) and comparison with present work.

4.2. Texture and Composition of Clinopyroxene

The texture and chemical composition of clinopyroxenes from the lavas of Flores, São Miguel, Terceira (Azores), Santo Antao (Cape Verde), and Lanzarote (Canary Islands) are reported. Clinopyroxenes occur as euhedral phenocrysts, varying in size from 0.2 to 1.0 mm, embedded in a glassy and cryptocrystalline groundmass.

In general, they are diopside [50], while only a few analyses from São Miguel and Playa Malva display a weak Ca depletion and can be classified as augite (Figure 9A–C). The Al_2O_3 content of clinopyroxene varies in the following ranges: Santo Antao (2.43–9.10

wt%), São Miguel (2.42–7.77 wt%), Flores (2.46–7.88 wt%), Terceira (2.58–3.82 wt%), Puerto Calero (4.39–9.27 wt%), and Playa Malva (1.60–5.00 wt%). The Al_2O_3 variation trends show a negative correlation with both SiO_2 ($R^2 = 0.93$) and MgO ($R^2 = 0.90$). Some clinopyroxenes in the lavas of Santo Antao are zoned, showing a marked increase in Al_2O_3 in the rims, which are in contact with the lava groundmass and Mg–Ca carbonates (Figure 10). The external border of the rim appears irregular and partially corroded, possibly hinting at a reaction with the lava. The clinopyroxene contains several minor elements, which vary as follows: TiO_2 (0.35–3.88 wt%), Cr_2O_3 (<1.32 wt%), Na_2O (0.3–1.36 wt%), and K_2O and MnO (<0.2 wt%). The TiO_2 content increases with increasing Al_2O_3 ($R^2 = 0.84$), while Cr_2O_3 increases with MgO , although with a more scattered correlation ($R^2 = 0.46$).

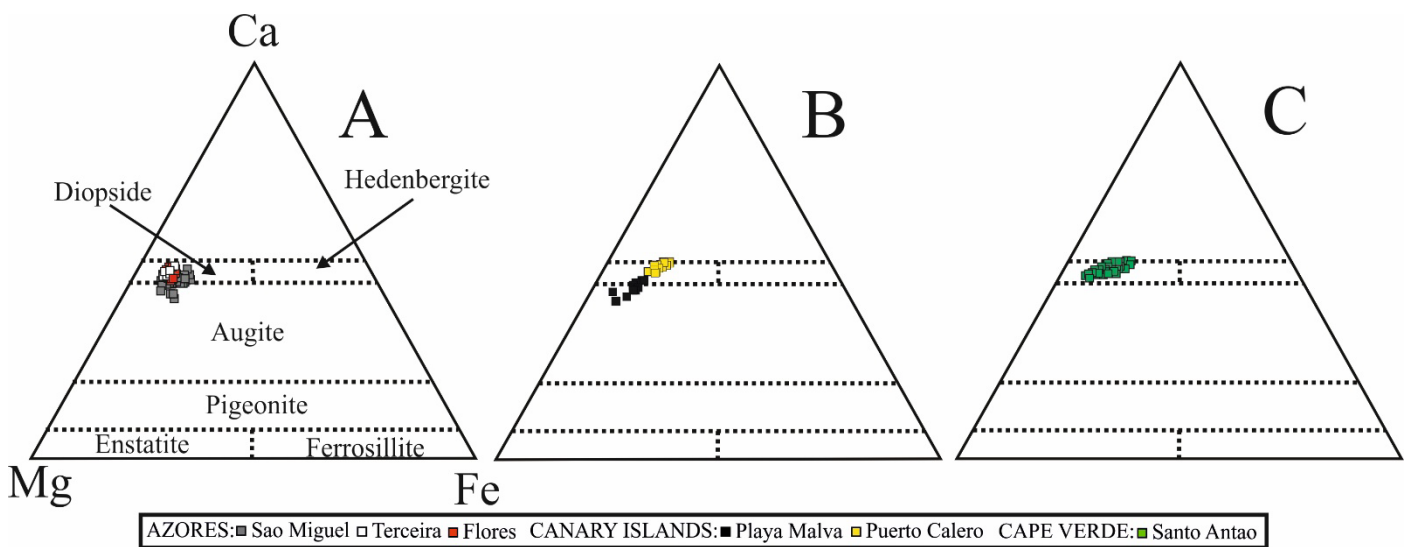


Figure 9. Classification of the analyzed clinopyroxene in the ternary diagram of Morimoto et al. [50]: (A) in the lavas of Azores, (B) in the basalts of Canaries, and (C) in the lavas of Cape Verde.

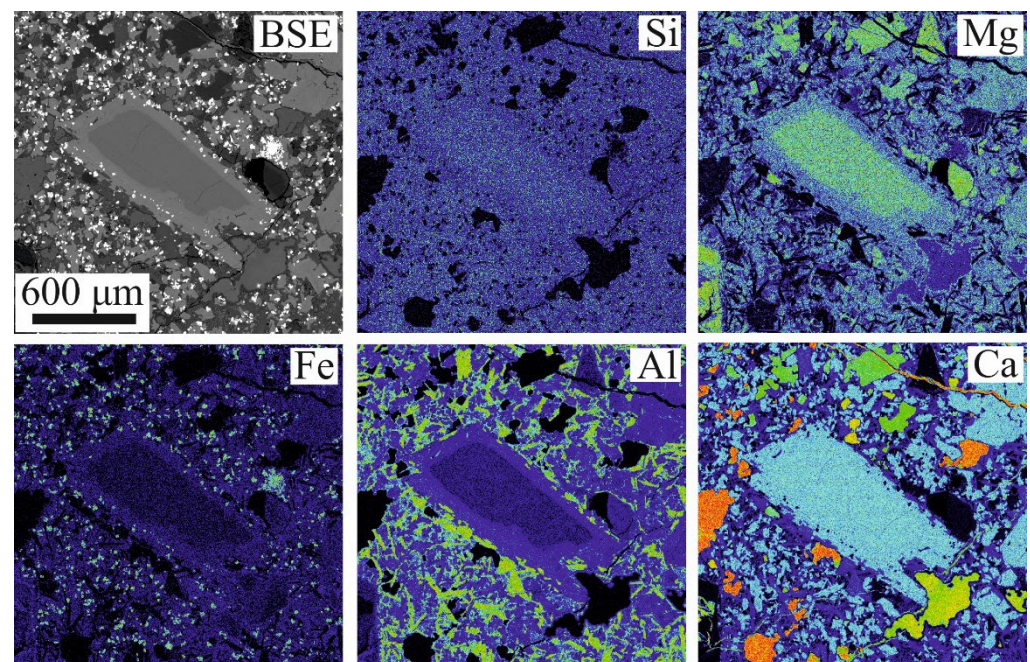


Figure 10. BSE image and X-ray element-distribution maps of Si, Mg, Fe, Al, and Ca in clinopyroxene from Santo Antao (Cape Verde) basalt. The spots enriched in Ca and Mg and Si-free are probably carbonates. Warm colors (yellow to red) denote high concentrations, cold colors (green to violet) denote low concentrations.

All the analyzed clinopyroxenes display (Ti + Cr) versus Ca relations, which are typical of non-orogenic lavas (Figure 11A). They also differ from tholeiites because of the relationships among Ti, (Ca + Na), and Al (Figure 11B), which are more consistent with alkali basalts [30,51]. All the analyzed clinopyroxenes show a negative correlation between Mg# and Ti apfu (Figure 11C). Clinopyroxene compositions are plotted in the TiO₂–SiO₂/100–Na₂O ternary diagram [6,29], which correlates the mineral chemistry of clinopyroxene with the geodynamic formation setting (Figure 12A–F). The entire dataset shows a certain affinity with within Oceanic Plate basalts (WOPBs) and Iceland basalts (ICBs). A small group of analyses, including the clinopyroxenes of Terceira (Azores) and Playa Blanca (Lanzarote, Canary Islands), display an unusual enrichment in Na₂O and plot out the proposed fields (Figure 12C,E).

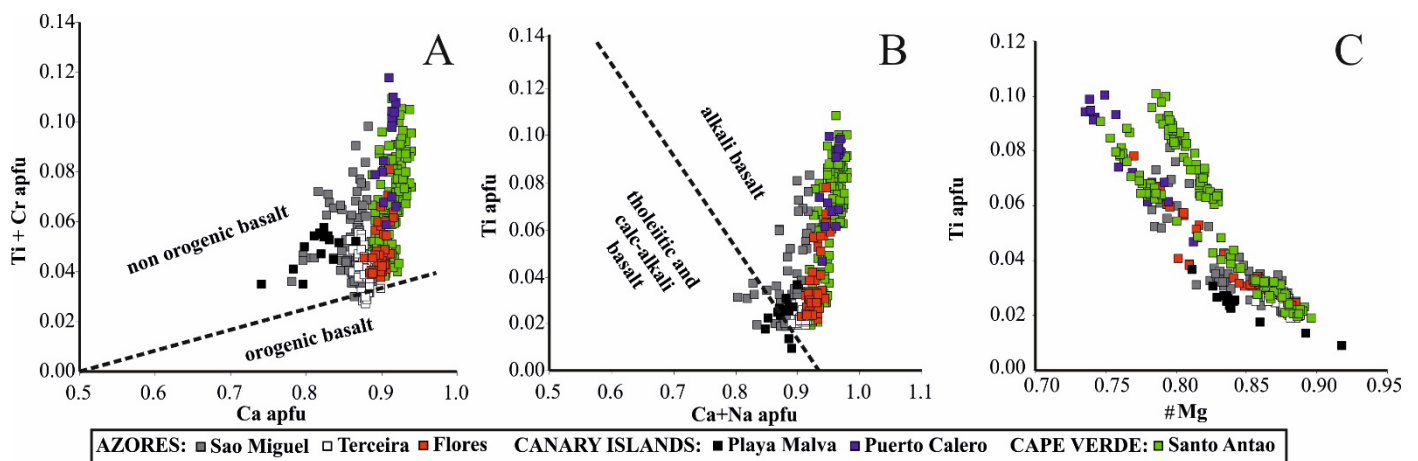


Figure 11. Compositional variation in the analyzed clinopyroxene in (A) Ca versus Ti + Cr, (B) Ca + Na versus Ti diagrams used to discriminate volcanic rocks of various magmatic types from various tectonic settings and (C) Mg# versus Ti. Modified after Letierrier et al. [30] and Ural [51].

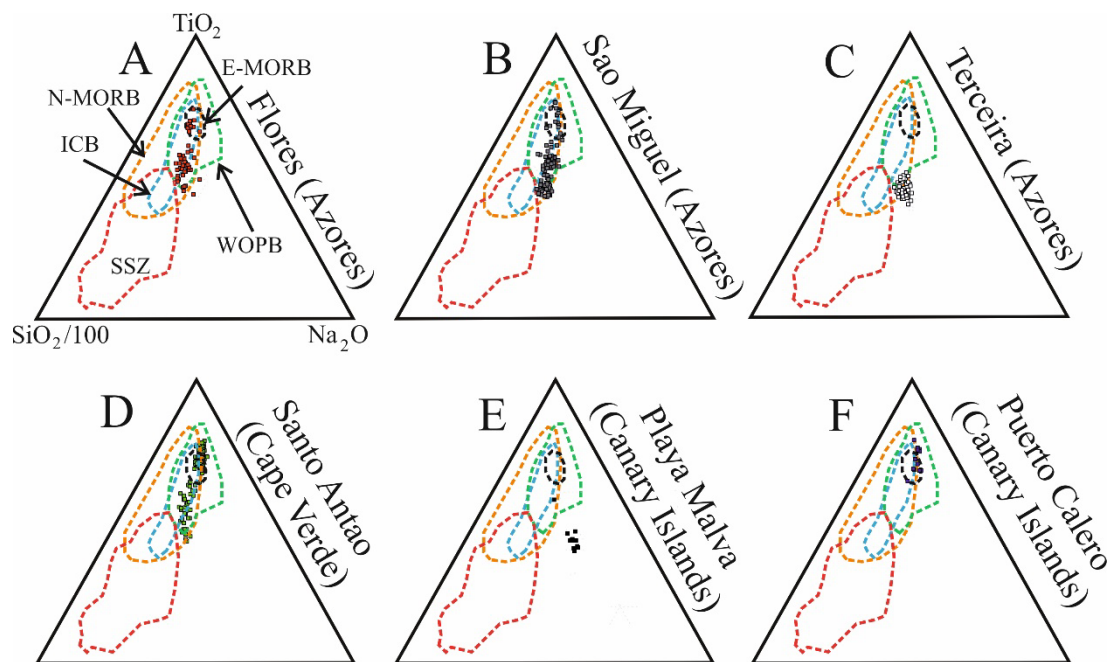


Figure 12. TiO₂–Na₂O–SiO₂/100 diagram for discriminating clinopyroxenes in basalts from different oceanic settings, modified after Beccaluva et al. [29] and Barbero et al. [6]: (A) in the basalt of Flores (Azores), (B) in the basalt of Sao Miguel (Azores), (C) in the basalt of Terceira (Azores), (D) in the basalt of Santo Antao (Cape Verde), (E) in the basalt of Playa Malva, Lanzarote, (Canary Islands) and (F) in the basalt of Puerto Calero, Lanzarote, (Canary Islands). Abbreviations: E-MORB =

enriched mid-ocean ridge basalt, N-MORB = normal mid-ocean ridge basalt, WOPB = within Oceanic Plate basalts, ICB = Iceland basalts, and SSZ = supra-subduction zone basalts.

4.3. Texture and Composition of Oxy-Spinel

Accessory grains of magmatic oxy-spinel have been analyzed in the lava of São Miguel (Azores), Santo Antao (Cape Verde), and in the dunite xenoliths of Playa Malva and Puerto Calero (Lanzarote, Canary Islands). Microscopically, the oxy-spinel forms euhedral crystals variable in size from 10 μm up to about 1 mm. In the lavas, oxy-spinel occurs disseminated in the glassy groundmass, in the contact between olivine phenocrysts and groundmass, and enclosed in olivine phenocrysts (Figure 13A–D). Oxy-spinel grains are usually fresh and occasionally show a narrow magnetite alteration rim and an irregular shape along the crystal boundaries in contact with the host lava (Figure 13C,D).

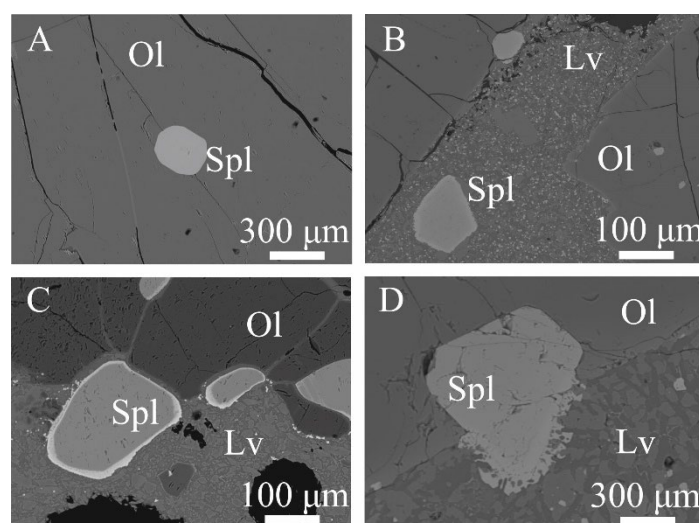


Figure 13. BSE images of accessory oxy-spinels in the studied samples. (A) Polyagonal grain enclosed in olivine from the Santo Antao lava, Cape Verde, (B) oxy-spinels in lava and in the contact lava–olivine from the xenolith of Playa Malva, Lanzarote, Canary Islands, (C) rounded grains of oxy-spinels rimmed with magnetite in the xenolith of Puerto Calero, Lanzarote, Canary Islands and (D) polyagonal grain of oxy-spinel occurring in the contact lava–olivine in the lava of Sao Miguel, Azores, showing an irregular rim in contact with lava. Abbreviations: Spl = oxy-spinel, Ol = olivine, Lv = lava.

Analyses of spinel grains are listed in Table S4 and plotted in the diagrams presented in Figure 14A–D. Based on the relationship between the chromium number [$\text{Cr}\# = \text{Cr}/(\text{Cr} + \text{Al})$] versus the magnesium number [$\text{Mg}\# = \text{Mg}/(\text{Mg} + \text{Fe}^{2+})$] [52], most of the analyzed oxy-spinel from São Miguel, Santo Antao, and Playa Malva corresponds to magnesiochromite, whereas the majority of oxy-spinel from Puerto Calero falls within the spinel field (Figure 14A). The chromium number of oxy-spinel is higher in the lavas ($\text{Cr}\# = 0.65\text{--}0.78$) compared to the xenoliths ($\text{Cr}\# = 0.42\text{--}0.56$). The Cr–Al– Fe^{3+} atomic ratios plotted in Figure 14B show a general Al–Cr substitution, although most of the analyzed oxy-spinels contain more than 50% of Cr (Figure 14B). Oxy-spinels analyzed in the lava from Sao Miguel, Santo Antao, and Madeira, and those in the xenoliths from Puerto Calero, Fuerteventura, and Sal, are enriched in Fe^{3+} (Figure 14B). No correlations are observed in the diagram Fe^{3+} number [$\text{Fe}^{3+\#} = \text{Fe}^{3+}/(\text{Fe}^{3+} + \text{Cr} + \text{Al})$] versus $\text{Mg}\#$ (Figure 14C). The content of TiO_2 ranges between 2.80–3.46 wt% and 2.47–4.92 wt% in the lava from São Miguel and Santo Antao, respectively, and varies from 0.26 to 0.35 wt% and 2.49 to 6.87 wt% in the xenoliths collected in Playa Malva and Puerto Calero, respectively (see Table S4).

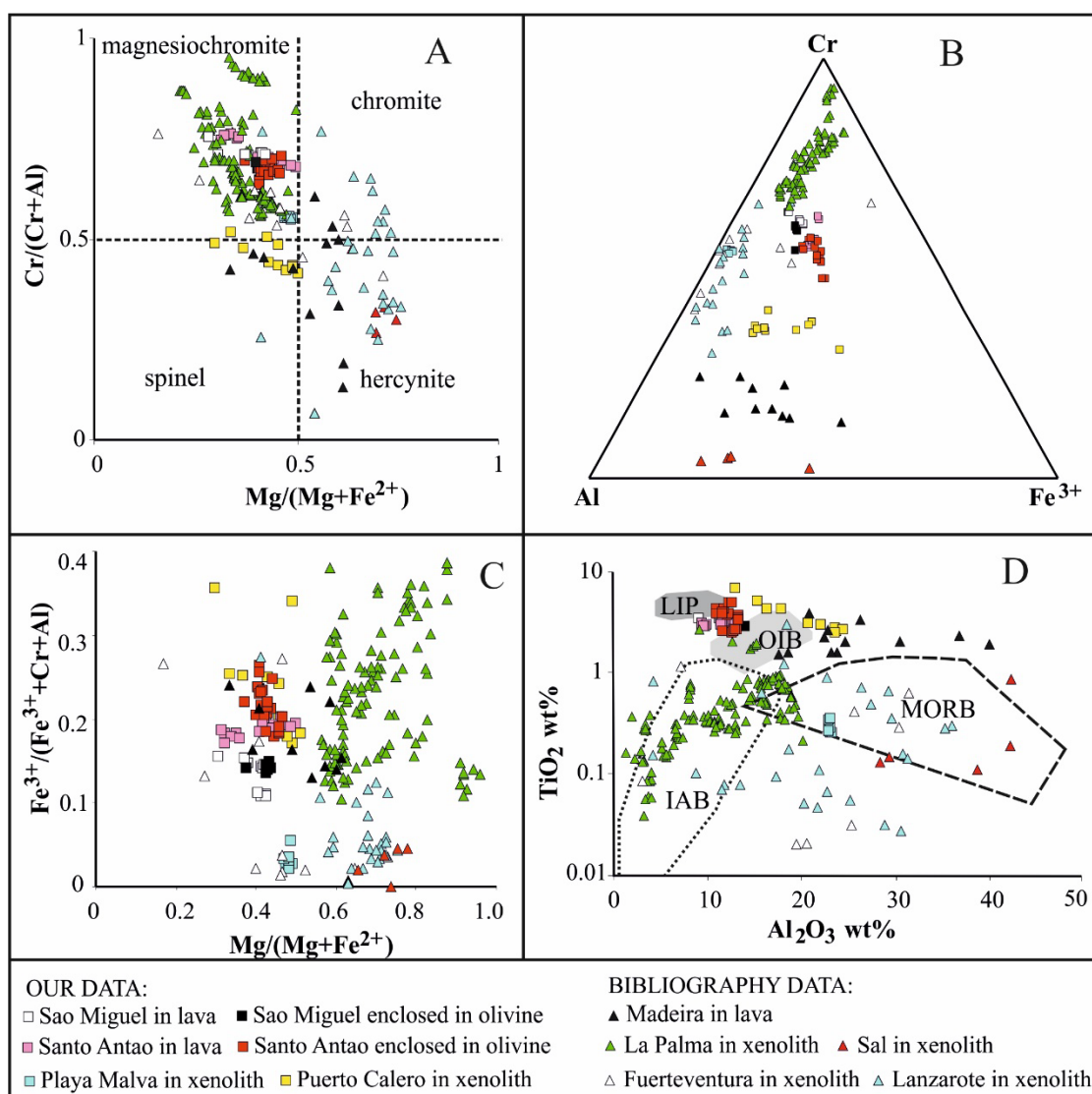


Figure 14. (A) Classification of the oxy-spinel from the studied samples and from literature (See Table S1) in the diagram $\text{Cr}/(\text{Cr} + \text{Al})$ versus $\text{Mg}/(\text{Mg} + \text{Fe}^{2+})$, from Bosi et al. [52], (B) Cr–Al– Fe^{3+} atomic ratios, (C) diagram $\text{Mg}/(\text{Mg} + \text{Fe}^{2+})$ versus $\text{Fe}^{3+}/(\text{Fe}^{3+} + \text{Cr} + \text{Al})$, (D) composition of the Macaronesia oxy-spinels, compared with the field of spinels from large igneous provinces (LIP) and oceanic island basalt (OIB), mid-ocean ridge basalt (MORB) and island arc basalt (IAB), fields from Dick and Bullen [3], Kamenetsky et al. [25] and Arai [53].

The amount of MnO is lower than 0.12 wt% in all analyzed oxy-spinels, with the exception of those hosted in the xenolith from Puerto Calero, in which it varies from 0.34–0.46 wt% (see Table S4). Other trace elements occur in negligible amounts ($\text{NiO} < 0.23$ wt%, $\text{ZnO} < 0.16$ wt%, $\text{V}_2\text{O}_5 < 0.29$ wt%).

A literature database referred to accessory oxy-spinel in peridotite xenoliths from La Palma, Fuerteventura, Lanzarote, and Sal [5,18,21,49] and oxy-spinel in alkaline basalts from Madeira [23]. Figure 14A shows that spinels from La Palma xenoliths are mostly magnesiochromite.

Their chromium number covers the entire variation range observed in magnesiochromite analyzed in this work. In contrast, the composition of oxy-spinels hosted within xenoliths from Fuerteventura ranges from magnesiochromite to chromite to rare hercynite, whereas magnesiochromite compositions apparently lack spinels from the Madeira alkaline basalts. In this case, the oxy-spinel composition varies from chromite to spinel and hercynite, with Mg# in the range of about 0.4–0.6.

On the basis of their compositions, all of the oxy-spinels from Sal xenoliths are classified as hercynite. Conversely, the oxy-spinels in the Lanzarote xenoliths analyzed by Neumann et al. [49] cover the entire compositional field (Figure 14A). The variation in TiO_2 versus Al_2O_3 in oxy-spinels can be used as an indicator of the tectonic setting of crystallization (Figure 14D) [3,25,53]. The oxy-spinels from Sao Miguel and Santao Antao lava and from the xenolith of Puerto Calero form a cluster around the fields of large igneous provinces (LIP) and oceanic island basalts (OIBs), whereas those of Playa Malva xenolith fall in the field of the mid-ocean ridge basalt (MORB) because of the relatively low TiO_2 content of Al_2O_3 , which is well above 20 wt% (Figure 14D).

On the basis of their compositions, all of the oxy-spinels from the Sal xenoliths are classified as hercynite. Conversely, the oxy-spinels in the Lanzarote xenoliths analyzed by Neumann et al. [49] cover the entire compositional field (Figure 14A).

A plot of the literature data shows that oxy-spinels analyzed in peridotite xenoliths from La Palma [5] have low TiO_2 and Al_2O_3 contents and are characteristic of island arc basalt (IABs), with only a few analyses entering the MORB and OIB fields (Figure 14D). Oxy-spinel from peridotite xenoliths of Fuerteventura are scattered either within the IAB and MORB compositional fields or a plot outside because of their low TiO_2 content. The oxy-spinels from Sal xenoliths show a compositional affinity with MORB spinels (Figure 14D). Analyses of spinels from the Lanzarote xenoliths [49] are characterized by a significant compositional variation, comprising both high and low TiO_2 and Al_2O_3 contents (Figure 14D). Lastly, the analyses from alkaline basalts of Madeira extend the compositional field of Macaronesian lava-hosted spinels to aluminum-rich compositions, similar to MORB but with much higher TiO_2 content, comparable to the OIB field.

4.4. Oxy-Spinel and Olivine Thermometry and Oxygen Barometry

Several pairs of oxy-spinel and olivine showing textural evidence of co-crystallization in the magmatic stage have been analyzed in the lava of São Miguel (Azores) and Santo Antao (Cape Verde) and in the peridotite xenoliths of Playa Malva and Puerto Calero (Lanzarote, the Canary Islands).

Thermobarometric data were calculated using the equations of Ballhaus et al. [54], assuming a constant pressure of 10 kbar. This value represents the upper limit of crystallization pressure for the Azores magma estimated by clinopyroxene geobarometry [55]. Although we are aware that oxy-spinel and olivine pairs may have crystallized at different pressures in lavas and xenoliths, dependence on the calculated temperature was minimal, as also observed by Mata and Munhá [23].

Oxy-spinel and olivine thermobarometric literature data available for alkaline basalts of Madeira [23] are in agreement with equilibration in a thermal range of 1205–721 °C, similar to that observed in our lava samples. However, the values of oxygen fugacity calculated for the alkaline basalts appear to be remarkably higher [$\Delta\log f(\text{O}_2)$ ranging between +0.9 and +2.4].

The oxygen fugacity is expressed as $\Delta\log f(\text{O}_2)$, i.e., a deviation from the Fayalite–Magnetite–Quartz (FMQ) buffer. The thermometry and oxygen barometry results have been listed in Table S5 and plotted in a binary diagram (Figure 15). The data show that olivine and spinel pairs in the lavas equilibrated in a wide range of temperatures from 1420° to 851 °C at a relatively high oxygen fugacity varying from -0.55 to $+1.19 \Delta\log f(\text{O}_2)$, which is thus well above the FMQ buffer in most cases.

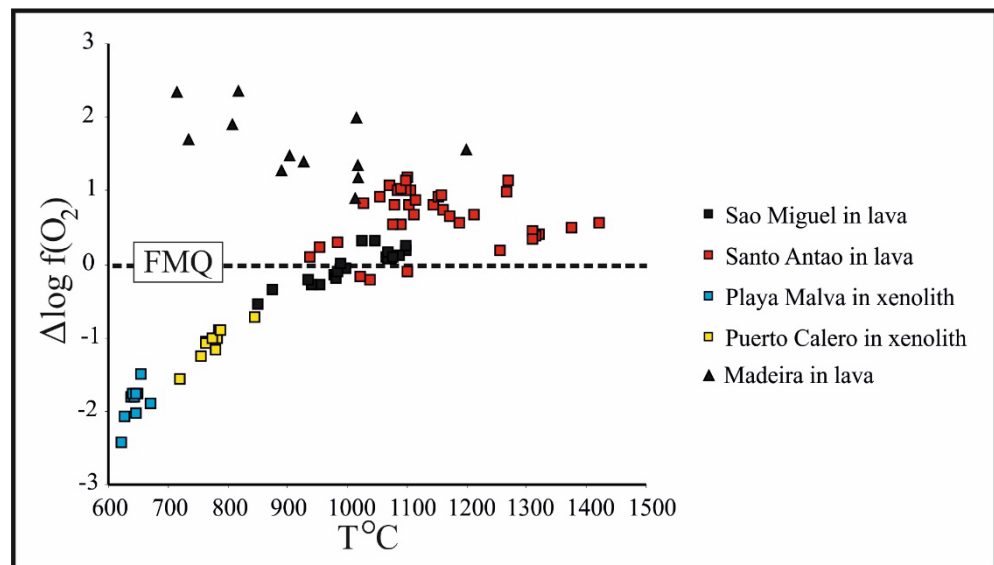


Figure 15. Oxygen fugacity and temperature calculated for olivine–spinel pairs from Sao Miguel and Santo Antao basalts, xenoliths from Playa Malva and Puerto Calero (present work and from basalts of Madeira [23]). The horizontal dashed line represents the Fayalite–Magnetite–Quartz (FMQ) buffer.

In contrast, olivine and spinel pairs from the peridotite xenoliths suggest equilibration at much lower temperatures (844–623 °C) and redox conditions varying from -2.43 to -0.71 $\Delta\log f(\text{O}_2)$, which are below the FMQ buffer.

5. Discussion

5.1. The Significance of Compositional Variations in Olivine

Olivine is a family of nesosilicates mainly composed of members of the forsterite–fayalite series, characterized by a general formula X_2TO_4 with $\text{X} = (\text{Mg}, \text{Fe})$ and $\text{T} = \text{Si}$ and Al , with a continuous Mg–Fe substitution.

Electron probe microanalysis has revealed that olivine may carry a number of trace elements (e.g., Ni, Mn, Co, Ca, Ti, Al, Cr, P, and Na) which have been widely used as indicators of chemical and thermodynamic conditions of olivine crystallization [56–66]. Our analyses and comparison with relevant literature data (Figures 6A–C, 7A–C, and 8A–I) show that the olivine of Macaronesian volcanic rocks and xenoliths mainly contain minor amounts of Ni, Mn, and Ca, attributable to a solid solution with structurally related end members of the “Olivine Group”, such as liebenbergite Ni_2SiO_4 , tephroite Mn_2SiO_4 , monticellite CaMgSiO_4 , and kirschsteinite CaFeSiO_4 [67].

Olivine present in the Macaronesia volcanic rocks is considered a co-genetic phenocryst that is precipitated early from the host lava and is thereby able to reflect compositional variations in the magma during its ascent to the surface.

The initial concentration of Mg, Fe, Ni, Mn, and Ca in the parent melt depends on the nature of the mantle source, which, in turn, is controlled by the mixing of variable proportions of primitive peridotitic mantle and recycled oceanic crust, as proposed for the Canary Islands’ mantle plume [17,58,68,69]. Olivine phenocrysts are progressively depleted in forsterite and Ni contents and enriched in Mn and Ca as a result of differentiation processes and the degree of compatibility of trace elements in the olivine structure [70–72]. This behavior accounts for the observed positive and negative correlation of Ni and Mn, respectively, with Fo% taken as the differentiation index of olivine (Figures 6B,C, 7B,C and 8D–I). The correlation of Ca appears more scattered compared to the differentiation trends of Ni and Mn due to an anomalous Ca-enrichment in olivine from the Azores, Cape Verde, and the Canary Islands (Figures 6A, 7A and 8A–C).

This feature, which is not fully consistent with magmatic differentiation, may be related to metasomatic processes in the mantle source of lavas [59]. The xenoliths associated with the volcanic rocks of Macaronesia represent fragments of country rocks taken up by the magma during an ascent to the surface and, therefore, did not crystallize in equilibrium with the host lava. The refractory composition ($Fo > 90\%$), the high Ni, and the low Mn and Ca contents of olivine in the dunite xenoliths of Lanzarote (Figure 6A–C) support the idea that they are fragments of residual mantle affected by a high degree of partial melting [73–75].

Conversely, most of the xenoliths from the Macaronesian archipelagos from the literature display a variegated lithology from dunite, harzburgite, and lherzolite to wehrlite and olivine gabbro (Table S1). Only a few samples contain olivine with a refractory composition similar to the dunite xenoliths of Lanzarote. In general, olivine shows a decrease in forsterite ($Fo = 90\text{--}45\%$) and Ni ($NiO = 0.65\text{--}0.0\text{ wt}\%$) from peridotites to gabbro, with a progressive enrichment in the incompatible Mn and Ca (Figure 8A–I). These correlation trends reflect a magmatic differentiation.

In agreement with other authors [14,26], we suggest that these xenoliths are fragments of igneous rocks formed by fractional crystallization and the cumulate formation of mafic melting in deep magma chambers. The anomalous high concentration of Ca ($Ca > 1500\text{ ppm}$) in olivine gabbro from the xenoliths of Tenerife and Corvo and few peridotites from Sal, Santa Maria, Fuerteventura, Lanzarote, and la Palma (Figure 8A–C) can be an effect of local metasomatism [18,22,26].

5.2. The Significance of Clinopyroxene Composition

Similar to olivine, clinopyroxene appears in the early phase during the crystallization of mantle-derived magmas. Therefore, the composition of magmatic clinopyroxene in volcanic rocks records key information regarding the chemistry and evolution of the host lavas, the crystallization conditions, and the geodynamic settings in which the clinopyroxene and its host rock formed [4,6,27,29,30,55,76]. In particular, it has been suggested that the variation in clinopyroxene compositions can be related to differences in the primary composition of the parent magma rather than the physical conditions of crystallization [77]. Furthermore, the composition of the lava can be inferred by the mineral chemistry of the host clinopyroxenes [4,30].

On the basis of their composition, euhedral shape, and the lack of development of abundant reaction rims, the studied clinopyroxenes can be classified as phenocrysts that crystallize in equilibrium with the host lava. The relationship between Al_2O_3 and TiO_2 is consistent with a magmatic differentiation process, as also observed in clinopyroxenes associated with igneous cumulates and lava from Fuerteventura [10].

Following the model proposed by Carracedo [34], we can argue that the clinopyroxenes analyzed in this contribution have been generated by fractional crystallization, which is very likely in a closed magmatic reservoir. On the basis of equilibrium diagrams proposed by Larrea et al. [14], the Cape Verde clinopyroxene analyzed in this contribution is probably crystallized from a more evolved magma.

Regarding the geodynamic environment of their formation, studied clinopyroxenes point to a preferential affinity to those precipitated in a divergent tectonic regime rather than a convergent one, such as a subduction zone (Figure 12A–F). This observation is also supported by the distribution of $Ti + Cr$ apfu versus Ca apfu (Figure 11A), which is fully consistent with clinopyroxenes reported from non-orogenic basalts [30,51]. Furthermore, the relationships among Ti , Ca , and Na (apfu) reported in Figure 11B,C suggest that the affinity of the clinopyroxene-hosting lava is incompatible with tholeiitic basalts and varies from alkaline to calc-alkaline basalts.

The slight enrichment in Na_2O observed in the clinopyroxenes from Terceira and Playa Malva samples (Figure 12C,E) can be attributed to a more alkaline signature of their host basalts, as suggested by Leterrier et al. [30].

5.3. The Significance of Oxy-Spinel Composition and Its Relationships with Co-Existing Olivine

Oxy-spinels are the most stable mantle minerals, and they are, in most cases, resistant to low-temperature secondary alteration processes. Therefore, their composition is a reliable petrogenetic tool often used to decipher the physico-chemical evolution of their host magmatic rocks (i.e., chemistry of parental magmas, degree of partial melting of the mantle source, etc.) and the geodynamic setting of their formation [3,25,53].

The composition of the oxy-spinels analyzed in the Macaronesian basalts and xenoliths (present work), and some from the Sal, Lanzarote, and Fuerteventura xenoliths Sal [5,18,21,49] plot in the OIB and MORB fields, suggest a common origin in an extensional regime (Figure 14D). Conversely, the oxy-spinels analyzed in xenoliths from La Palma [5] fall in the field of the IAB, which is typical of convergent tectonic plate boundaries associated with a subduction zone (Figure 14D). These data are in contrast with the fact that the Macaronesia volcanic islands are mantle-plume-related; thus, the compositional variation in the unaltered magmatic oxy-spinels associated with the analyzed lava can be attributed to mantle heterogeneity.

In particular, the affinity of the oxy-spinels from La Palma can be explained by the model based on a multi-isotopic and geochemical study proposed by Day et al. [69], in which the assimilation of variable portions of recycled components, including subducted oceanic crust and lithosphere, played an important role in generating the OIB signatures typical of the Canaries.

Alternatively, we suggest that, in the studied case, the composition of the oxy-spinels is not exhaustive to decipher the geodynamic setting and the magma affinity in which they are crystallized. Natural observations and experimental data have shown that co-existing oxy-spinel and olivine adjust their Mg–Fe ratios by a diffusion–exchange reaction after the magmatic crystallization stage, depending on temperature, oxygen fugacity, chromite–olivine mass ratio, dissolution, and the cooling rate ([2,54,78–81] and references therein), allowing the calculation of temperature and oxygen fugacity for the reaction [2,54].

The equilibration involves the diffusion of Fe from the silicate to the oxide and, at a constant spinel–olivine mass ratio, is favored by a slow cooling rate or is inhibited if cooling is rapid (quenching). Although the obtained results (Table S5) may be unrealistic as absolute values, they are meaningful in the relative sense, showing a clear distinction between the spinel–olivine pairs in basaltic lavas from Sao Miguel, Santo Antao (present work), and Madeira [23] and from those in the mantle xenoliths from Playa Malva and Puerto Calero (Figure 15). The indication is that, in the lavas, the equilibration closed soon after the spinel–olivine co-crystallization in a wide thermal range of 1420–851 °C, in contrast to the mantle xenoliths, in which the system closed at lower temperatures between 844 and 623 °C (Figure 15).

This observation would be consistent with a rapid cooling rate in the spinel–olivine pairs of the lavas compared with the mantle xenoliths, which crystallized at depth, with equilibration lasting longer and probably extending to lower temperatures as well. The data also indicate that spinel and olivine in basaltic lavas crystallized at higher oxygen fugacity compared to those in mantle xenoliths (Figure 15). The calculated values agree with the conclusion that the majority of mantle-derived magmas are initially highly reduced and reached relatively oxidized values on the surface [82].

6. Summary and Concluding Remarks

The Macaronesian archipelagos are interpreted as separate submarine seamount volcanoes built up by the extrusion of magma at hotspots related to the emplacement of mantle plumes into the sub-oceanic lithosphere of the North Atlantic Ocean [34,35].

In view of this model, the mineral chemistries of olivine, clinopyroxene, and oxy-spinel obtained in this work, along with a comparison of available literature data, provide enough information to constrain some aspects concerning the origin, evolution, and

crystallization conditions of Macaronesian volcanic rocks. In particular, the data allow the following conclusions to be drawn:

(1) The validity of the mineral chemistry of olivine, clinopyroxene, and oxy-spinel as petrogenetic tracers is confirmed, representing a powerful tool for the geodynamic analysis of volcanic magmatic systems and the magma composition and evolution.

(2) Using the selected analytical conditions, we have successfully discriminated the origin of olivine, i.e., crystallized in the lithospheric mantle or in volcanic rocks. Olivine analyzed in Lanzarote dunite xenoliths, which represent fragments of solid mantle transported by the host lava, exhibits higher and relatively fixed Fo% values and a different distribution of the minor elements Ca, NiO, and MnO compared to the olivine occurring as phenocrysts in basalts from the Macaronesia archipelagos.

(3) Literature data show a wider variation in the MgO–FeO ratio in gabbro olivine and in a few peridotite xenoliths from Macaronesia compared to those analyzed in this contribution. This variation was attributed to (1) a fractional crystallization process that started in a deep magma chamber, suggesting that these xenoliths represent a portion of cumulate rocks and not fragments of mantle, and (2) they were affected by the interaction with metasomatic fluids.

(4) The mineral chemistry of clinopyroxene phenocrysts was used to decipher the geotectonic environment of the formation of the host basalt and suggests that the analyzed clinopyroxenes were crystallized in an extensional regime. Since the composition of clinopyroxene is closely related to host rock bulk chemistry, the lavas hosting the analyzed clinopyroxenes have an alkaline signature. Furthermore, their euhedral morphology and composition suggest that the studied clinopyroxenes were formed by fractional crystallization in a closed magmatic reservoir.

(5) The composition of the oxy-spinels analyzed in the Macaronesia basalts and xenoliths prevents us from drawing solid conclusions regarding the geodynamic environment of their formation. Nevertheless, the relationship between oxy-spinel and olivine in equilibrium was successfully used as an oxybarometer and geothermometer, showing evidence that the basalts were crystallized from a melt with higher oxygen fugacity compared to those of the mantle xenoliths and with a different cooling history since the mantle xenoliths crystallized and reached the equilibrium more slowly than the basalts.

Supplementary Materials: The following supporting information can be downloaded at <https://www.mdpi.com/article/10.3390/min14020161/s1>, Table S1. Description of the samples from Macaronesia overviewed in this work; Table S2. Electron microprobe analyses of olivine from Macaronesia; Table S3. Electron microprobe analyses of clinopyroxene from Macaronesia; Table S4. Electron microprobe analyses of oxy-spinel from Macaronesia; Table S5. Result of thermometry and oxygen barometry.

Author Contributions: Bibliographic research, conceptualization and data curation, F.Z., G.G., R.M., C.M., P.V., A.P. and S.N.; Sampling, F.Z., G.G., R.M., A.P. and S.N.; Data collection, F.Z.; Writing—original draft preparation, F.Z.; Writing—review and editing, F.Z., G.G., R.M., C.M., P.V., A.P. and S.N. All authors have read and agreed to the published version of the manuscript.

Funding: This research did not receive external funding.

Data Availability Statement: The original data presented in the study are included in the article as Supplementary Materials.

Acknowledgments: The manuscript benefited greatly from critical reviews by anonymous reviewers.

Conflicts of Interest: The authors declare no conflicts of interest.

References

1. Jollands, M.C.; Dohmen, R.; Padrón-Navarta, J.A. Hide and Seek—Trace Element Incorporation and Diffusion in Olivine. *Elements* **2023**, *19*, 144–150.
2. Garuti, G.; Pushakarev, E.V.; Thalhammer, O.A.; Zaccarini, F. Chromitites of the Urals (part 1): Overview of chromite mineral chemistry and geo-tectonic setting. *Ofioliti* **2012**, *37*, 27–53.
3. Dick, H.J.; Bullen, T. Chromian spinel as a petrogenetic indicator in abyssal and alpine-type peridotites and spatially associated lavas. *Contrib. Mineral. Petrol.* **1984**, *86*, 54–76.
4. Nisbet, E.G.; Pearce, J.A. Clinopyroxene composition in mafic lavas from different tectonic settings. *Contrib. Mineral. Petrol.* **1977**, *63*, 149–160.
5. Klügel, A.; Albers, E.; Hansteen, T.H. Mantle and crustal xenoliths in a tephriphonolite from La Palma (Canary Islands): Implications for phonolite formation at Oceanic Island volcanoes. *Front. Earth Sci.* **2022**, *10*, 761902.
6. Barbero, E.; Delavari, M.; Dolati, A.; Vahedi, L.; Langone, A.; Marroni, M.; Pandolfi, L.; Zaccarini, F.; Saccani, E. Early Cretaceous Plume–Ridge Interaction Recorded in the Band-e-Zeyarat Ophiolite (North Makran, Iran): New Constraints from Petrological, Mineral Chemistry, and Geochronological Data. *Minerals* **2020**, *10*, 1100.
7. Rogkala, A.; Petrounias, P.; Tsikouras, B.; Giannakopoulou, P.P.; Hatzipanagiotou, K. Mineralogical evidence for partial melting and melt-rock interaction processes in the mantle peridotites of Edessa ophiolite (North Greece). *Minerals* **2019**, *9*, 120.
8. Taracsák, Z.; Hartley, M.; Burgess, R.; Edmonds, M.; Iddon, F.; Longpré, M. High fluxes of deep volatiles from ocean island volcanoes: Insights from El Hierro, Canary Islands. *Geochim. Cosmochim. Acta* **2019**, *258*, 19–36.
9. Gómez-Ulla, A.; Sigmarsson, O.; Gudfinnsson, G.H. Trace element systematics of olivine from historical eruptions of Lanzarote, Canary Islands: Constraints on mantle source and melting mode. *Chem. Geol.* **2017**, *449*, 99–111.
10. Tornare, E.; Pilet, S.; Bussy, F. Magma differentiation in vertical conduits revealed by the complementary study of plutonic and volcanic rocks from Fuerteventura (Canary Islands). *J. Petrol.* **2016**, *57*, 2221–2250.
11. Albert, H.; Costa, F.; Martí, J. Timing of magmatic processes and unrest associated with mafic historical monogenetic eruptions in Tenerife Island. *J. Petrol.* **2015**, *56*, 1945–1966.
12. Barker, A.; Holm, P.M.; Troll, V. The role of eclogite in the mantle heterogeneity at Cape Verde. *Contrib. Mineral. Petrol.* **2014**, *168*, 1052.
13. Gurenko, A.A.; Geldmacher, J.; Hoernle, K.A.; Sobolev, A.V. A composite, isotopically-depleted peridotite and enriched pyroxenite source for Madeira magmas: Insights from olivine. *Lithos* **2013**, *170*, 224–238.
14. Larrea, P.; França, Z.; Lago, M.; Widom, E.; Galé, C.; Ubide, T. Magmatic processes and the role of antecrysts in the genesis of Corvo Island (Azores Archipelago, Portugal). *J. Petrol.* **2013**, *54*, 769–793.
15. Gurenko, A.A.; Bindeman, I.N.; Chaussidon, M. Oxygen isotope heterogeneity of the mantle beneath the Canary Islands: Insights from olivine phenocrysts. *Contrib. Mineral. Petrol.* **2011**, *162*, 349–363.
16. Gurenko, A.A.; Hoernle, K.A.; Sobolev, A.V.; Hauff, F.; Schmincke, H.U. Source components of the Gran Canaria (Canary Islands) shield stage magmas: Evidence from olivine composition and Sr–Nd–Pb isotopes. *Contrib. Mineral. Petrol.* **2010**, *159*, 689–702.
17. Gurenko, A.A.; Sobolev, A.V.; Hoernle, K.A.; Hauff, F.; Schmincke, H.U. Enriched, HIMU-type peridotite and depleted recycled pyroxenite in the Canary plume: A mixed-up mantle. *Earth Planet. Sci. Lett.* **2009**, *277*, 514–524.
18. Abu El-Rus, M.A.; Neumann, E.R.; Peters, V. Serpentinization and dehydration in the upper mantle beneath Fuerteventura (eastern Canary Islands): Evidence from mantle xenoliths. *Lithos* **2006**, *89*, 24–46.
19. Gurenko, A.; Hoernle, K.; Hauff, F.; Schmincke, H.U.; Han, D.; Miura, Y.; Kaneoka, I. Major, trace element and Nd–Sr–Pb–O–He–Ar isotope signatures of shield stage lavas from the central and western Canary Islands: Insights into mantle and crustal processes. *Chem. Geol.* **2006**, *233*, 75–112.
20. Holm, P.; Wilson, J.; Christensen, B.; Hansen, L.; Hansen, S.; Hein, K.; Mortensen, A.; Pedersen, R.; Plesner, S.; Runge, M. Sampling the Cape Verde mantle plume: Evolution of melt compositions on Santo Antão, Cape Verde Islands. *J. Petrol.* **2006**, *47*, 145–189.
21. Shaw, C.S.; Heidelbach, F.; Dingwell, D.B. The origin of reaction textures in mantle peridotite xenoliths from Sal Island, Cape Verde: The case for “metasomatism” by the host lava. *Contrib. Mineral. Petrol.* **2006**, *151*, 681–697.
22. Neumann, E.R.; Griffin, W.L.; Pearson, N.J.; O’Reilly, S.Y. The evolution of the upper mantle beneath the Canary Islands: Information from trace elements and Sr isotope ratios in minerals in mantle xenoliths. *J. Petrol.* **2004**, *45*, 2573–2612.
23. Mata, J.; Munhá, J. Madeira Island alkaline lava spinels: Petrogenetic implications. *Mineral. Petrol.* **2004**, *81*, 85–111.
24. Neumann, E.R.; Wulff-Pedersen, E.; Pearson, N.; Spencer, E. Mantle xenoliths from Tenerife (Canary Islands): Evidence for reactions between mantle peridotites and silicic carbonatite melts inducing Ca metasomatism. *J. Petrol.* **2002**, *43*, 825–857.
25. Kamenetsky, V.S.; Crawford, A.J.; Meffre, S. Factors controlling chemistry of magmatic spinel: An empirical study of associated olivine, Cr-spinel and melt inclusions from primitive rocks. *J. Petrol.* **2001**, *42*, 655–671.
26. Neumann, E.R.; Sørensen, V.; Simonsen, S.; Johnsen, K. Gabbroic xenoliths from La Palma, Tenerife and Lanzarote, Canary Islands: Evidence for reactions between mafic alkaline Canary Islands melts and old oceanic crust. *J. Volcanol. Geotherm. Res.* **2000**, *103*, 313–342.
27. Soesoo, A. A multivariate statistical analysis of clinopyroxene composition: Empirical coordinates for the crystallisation PT-estimations. *GFF* **1997**, *119*, 55–60.

28. Mattioli, M.; Upton, J.; Renzulli, A.. Sub-volcanic crystallization at Sete Cidades volcano, São Miguel, Azores, inferred from mafic and ultramafic plutonic nodules. *Mineral. Petrol.* **1997**, *60*, 1.
29. Beccaluva, L.; Macciotta, G.; Piccardo, G.; Zeda, O. Clinopyroxene composition of ophiolite basalts as petrogenetic indicator. *Chem. Geol.* **1989**, *77*, 165–182.
30. Leterrier, J.; Maury, R.C.; Thonon, P.; Girard, D.; Marchal, M. Clinopyroxene composition as a method of identification of the magmatic affinities of paleo-volcanic series. *Earth Planet. Sci. Lett.* **1982**, *59*, 139–154.
31. Schweitzer, E.; Papike, J.; Bence, A. Statistical analysis of clinopyroxenes from deep-sea basalts. *Am. Mineral.* **1979**, *64*, 501–513.
32. Boone, G.M.; Fernandez, L.A. Phenocrystic olivines from the eastern Azores. *Mineral. Mag.* **1971**, *38*, 165–178.
33. Pimentel, A.; Ramalho, R.S.; Becerril, L.; Larrea, P.; Brown, R.J. Ocean island volcanoes: Genesis, evolution and Impact. *Front. Earth Sci.* **2020**, *8*, 82.
34. Carracedo, J.C. Growth, structure, instability and collapse of Canarian volcanoes and comparisons with Hawaiian volcanoes. *J. Volcanol. Geotherm. Res.* **1999**, *94*, 1–19.
35. Carracedo, J.C.; Troll, V.R. *North-East Atlantic Islands: The Macaronesian Archipelagos*; Elsevier: Amsterdam, The Netherlands, 2021; pp. 674–699, ISBN 978-0-12-809663-5.
36. Madeira, J.; Brum da Silveira, A.; Hipólito, A.; Carmo, R.; Gaspar, J.; Guest, J.; Duncan, A.; Barriga, F.; Chester, D. Active tectonics along the Eurasia-Nubia boundary: Data from the central and eastern Azores Islands. *Volcan. Geol. São Miguel Isl. Azores Archipel. Geol. Soc. Lond. Mem.* **2015**, *44*, 15–32.
37. Miranda, J.; Luis, J.; Lourenço, N.; Goslin, J. Distributed deformation close to the Azores Triple “Point”. *Mar. Geol.* **2014**, *355*, 27–35.
38. Lourenço, N.; Miranda, J.; Luis, J.; Ribeiro, A.; Victor, L.M.; Madeira, J.; Needham, H. Morpho-tectonic analysis of the Azores Volcanic Plateau from a new bathymetric compilation of the area. *Mar. Geophys. Res.* **1998**, *20*, 141–156.
39. Ramalho, R.S.; Helffrich, G.; Madeira, J.; Cosca, M.; Thomas, C.; Quartau, R.; Hipólito, A.; Rovere, A.; Hearty, P.J.; Ávila, S.P. Emergence and evolution of Santa Maria Island (Azores)—The conundrum of uplifted islands revisited. *Geol. Soc. Am. Bull.* **2017**, *129*, 372–390.
40. Demande, J.; Fabriol, R.; Gerard, F.; Lundt, F.; Chovelon, P. *Prospection Géothermique, Iles de Faial et de Pico (Açores). Rapport Géologique, Geochimique et Gravimétrique*; BRGM: Orléans, France, 1982, 65p.
41. Cannat, M.; Briais, A.; Deplus, C.; Escartin, J.; Georgen, J.; Lin, J.; Mercouriev, S.; Meyzen, C.; Muller, M.; Pouliquen, G.; et al. Mid-Atlantic Ridge–Azores hotspot interactions: Along-axis migration of a hotspot-derived event of enhanced magmatism 10 to 4 Ma ago. *Earth Planet. Sci. Lett.* **1999**, *173*, 257–269.
42. Gente, P.; Dymant, J.; Maia, M.; Goslin, J. Interaction between the Mid-Atlantic Ridge and the Azores hot spot during the last 85 Myr: Emplacement and rifting of the hot spot-derived plateaus. *Geochem. Geophys. Geosyst.* **2003**, *4*. <https://doi.org/10.1029/2003GC000527>.
43. Storch, B.; Haase, K.; Romer, R.; Beier, C.; Koppers, A. Rifting of the oceanic Azores Plateau with episodic volcanic activity. *Sci. Rep.* **2020**, *10*, 19718.
44. Larrea, P.; França, Z.; Widom, E.; Lago, M. Petrology of the Azores Islands. In *Volcanoes of the Azores—Revealing the Geological Secrets of the Central Northern Atlantic Islands*; Active Volcanoes of the World Series; Kueppers, U., Beier, C., Eds.; Springer: Berlin/Heidelberg, Germany, 2018; pp. 197–249, ISBN 978-3662585467.
45. Andrade, M.; Pimentel, A.; Ramalho, R.; Kutterolf, S.; Hernández, A. The recent volcanism of Flores Island (Azores): Stratigraphy and eruptive history of Funda Volcanic System. *J. Volcanol. Geotherm. Res.* **2022**, *432*, 107706.
46. Self, S. The recent volcanology of Terceira, Azores. *J. Geol. Soc.* **1976**, *132*, 645–666.
47. Plesner, S.; Holm, P.; Wilson, J. ⁴⁰Ar–³⁹Ar geochronology of Santo Antão, Cape Verde Islands. *J. Volcanol. Geotherm. Res.* **2003**, *120*, 103–121.
48. Weis, F.A.; Skogby, H.; Troll, V.R.; Deegan, F.M.; Dahren, B. Magmatic water contents determined through clinopyroxene: Examples from the Western Canary Islands, Spain. *Geochem. Geophys. Geosystems* **2015**, *16*, 2127–2146.
49. Neumann, E.R.; Wulff-Pedersen, E.; Johnsen, K.; Andersen, T.; Krogh, E. Petrogenesis of spinel harzburgite and dunite suite xenoliths from Lanzarote, eastern Canary Islands: Implications for the upper mantle. *Lithos* **1995**, *35*, 83–107.
50. Morimoto, N.; Fabries, J.; Ferguson, A.K.; Ginzburg, I.V.; Ross, M.; Seifert, F.A.; Zussman, J.; Aoki, K.; Gottardi, G. Nomenclature of pyroxenes. *Am. Mineral.* **1988**, *73*, 1123–1133.
51. Ural, M. Major and Trace Element Compositions of Clinopyroxene Phenocrysts in Altered Basaltic Rocks from Yükseskova Complex within Bitlis Suture Zone (Elazığ, Eastern Turkey): Implications for the Tholeiitic to Calc-Alkaline Magmatism. *Minerals* **2023**, *13*, 266.
52. Bosi, F.; Biagioni, C.; Pasero, M. Nomenclature and classification of the spinel supergroup. *Eur. J. Mineral.* **2019**, *31*, 183–192.
53. Arai, S. Chemistry of chromian spinel in volcanic rocks as a potential guide to magma chemistry. *Mineral. Mag.* **1992**, *56*, 173–184.
54. Ballhaus, C.; Berry, R.; Green, D. High-pressure experimental calibration of the olivine-orthopyroxene-spinel oxygen geobarometer: Implications for the oxidation state of the upper mantle. *Contrib. Mineral. Petrol.* **1994**, *118*, 109.
55. Nazzareni, S.; Barbarossa, V.; Skogby, H.; Zanon, V.; Petrelli, M. Magma water content of Pico Volcano (Azores Islands, Portugal): A clinopyroxene perspective. *Contrib. Mineral. Petrol.* **2020**, *175*, 87. <https://doi.org/10.1007/s00410-020-01728-7>.
56. Batanova, V.G.; Sobolev, A.V.; Kuzmin, D.V. Trace element analysis of olivine: High precision analytical method for JEOL JXA-8230 electron probe microanalyser. *Chem. Geol.* **2015**, *419*, 149–157.

57. Jiang, P.; Perfit, M.; Foster, D.A.; Trucco, A. Accurate analyses of key petrogenetic minor and trace elements in olivine by electron microprobe. *Chem. Geol.* **2022**, *614*, 121199.
58. Sobolev, A.V.; Hofmann, A.W.; Kuzmin, D.V.; Yaxley, G.M.; Arndt, N.T.; Chung, S.L.; Danyushevsky, L.V.; Elliott, T.; Frey, F.A.; Garcia, M.O.; et al. The amount of recycled crust in sources of mantle-derived melts. *Science* **2007**, *316*, 412–417.
59. Foley, S.F.; Prelevic, D.; Rehfeldt, T.; Jacob, D.E. Minor and trace elements in olivines as probes into early igneous and mantle melting processes. *Earth Planet. Sci. Lett.* **2013**, *363*, 181–191.
60. Putirka, K.; Tao, Y.; Hari, K.; Perfit, M.R.; Jackson, M.G.; Arevalo, R. The mantle source of thermal plumes: Trace and minor elements in olivine and major oxides of primitive liquids (and why the olivine compositions don't matter). *Am. Mineral.* **2018**, *103*, 1253–1270.
61. De Hoog, J.C.; Gall, L.; Cornell, D.H. Trace-element geochemistry of mantle olivine and application to mantle petrogenesis and geothermobarometry. *Chem. Geol.* **2010**, *270*, 196–215.
62. Shea, T.; Hammer, J.E.; Hellebrand, E.; Mourey, A.J.; Costa, F.; First, E.C.; Lynn, K.J.; Melnik, O. Phosphorus and aluminum zoning in olivine: Contrasting behavior of two nominally incompatible trace elements. *Contrib. Mineral. Petrol.* **2019**, *174*, 85. <https://doi.org/10.1007/s00410-019-1618-y>.
63. Mavrogenatos, K.; Flemetakis, S.; Papoutsas, A.; Klemme, S.; Berndt, J.; Economou, G.; Pantazidis, A.; Baziotis, I.; Asimow, P. Phosphorus zoning from secondary olivine in mantle xenolith from Middle Atlas mountains (Morocco, Africa): Implications for crystal growth kinetics. *Bull. Geol. Soc. Greece* **2016**, *50*, 1923–1932.
64. Wang, J.; Su, B.X.; Robinson, P.T.; Xiao, Y.; Bai, Y.; Liu, X.; Sakyi, P.A.; Jing, J.J.; Chen, C.; Liang, Z.; et al. Trace elements in olivine: Proxies for petrogenesis, mineralization and discrimination of mafic-ultramafic rocks. *Lithos* **2021**, *388*, 106085.
65. Jennings, E.S.; Gibson, S.A.; Maclennan, J. Hot primary melts and mantle source for the Paraná-Etendeka flood basalt province: New constraints from Al-in-olivine thermometry. *Chem. Geol.* **2019**, *529*, 119287.
66. Su, B.; Chen, Y.; Mao, Q.; Zhang, D.; Jia, L.H.; Guo, S. Minor elements in olivine inspect the petrogenesis of orogenic peridotites. *Lithos* **2019**, *344*, 207–216.
67. Back, M.E. *Fleischer's Glossary of Mineral Species*; Mineralogical Record, Mineralogical Association of Canada: Québec, QC, Canada, 2018.
68. Day, J.M.; Pearson, D.G.; Macpherson, C.G.; Lowry, D.; Carracedo, J.C. Pyroxenite-rich mantle formed by recycled oceanic lithosphere: Oxygen-osmium isotope evidence from Canary Island lavas. *Geology* **2009**, *37*, 555–558.
69. Day, J.M.; Pearson, D.G.; Macpherson, C.G.; Lowry, D.; Carracedo, J.C. Evidence for distinct proportions of subducted oceanic crust and lithosphere in HIMU-type mantle beneath El Hierro and La Palma, Canary Islands. *Geochim. Cosmochim. Acta* **2010**, *74*, 6565–6589.
70. Hart, S.R.; Davis, K.E. Nickel partitioning between olivine and silicate melt. *Earth Planet. Sci. Lett.* **1978**, *40*, 203–219.
71. Beattie, P.; Ford, C.; Russell, D. Partition coefficients for olivine-melt and orthopyroxene-melt systems. *Contrib. Mineral. Petrol.* **1991**, *109*, 212–224.
72. Wang, Z.; Gaetani, G.A. Partitioning of Ni between olivine and siliceous eclogite partial melt: Experimental constraints on the mantle source of Hawaiian basalts. *Contrib. Mineral. Petrol.* **2008**, *156*, 661–678.
73. Li, C.; Thakurta, J.; Ripley, E.M. Low-Ca contents and kink-banded textures are not unique to mantle olivine: Evidence from the Duke Island Complex, Alaska. *Mineral. Petrol.* **2012**, *104*, 147–153.
74. Day, J.M. Noble gas isotope systematics in the Canary Islands and implications for refractory mantle components. *Geochim. Cosmochim. Acta* **2022**, *331*, 35–47.
75. Simon, N.S.; Neumann, E.R.; Bonadiman, C.; Coltorti, M.; Delpech, G.; Grégoire, M.; Widom, E. Ultra-refractory domains in the oceanic mantle lithosphere sampled as mantle xenoliths at ocean islands. *J. Petrol.* **2008**, *49*, 1223–1251.
76. Nazzareni, S.; Morgavi, D.; Petrelli, M.; Bartoli, O.; Perugini, D. Magmatic processes at Euganean Hills (Veneto Volcanic Province, Italy): Clinopyroxene investigation to unravel magmatic interactions. *Geosciences* **2022**, *12*, 108.
77. Capedri, S.; Venturelli, G. Clinopyroxene composition of ophiolitic metabasalts in the Mediterranean area. *Earth Planet. Sci. Lett.* **1979**, *43*, 61–73.
78. Engi, M. Equilibria involving Al-Cr spinel: Mg-Fe exchange with olivine. Experiments, thermodynamic analysis, and consequences for geothermometry. *Am. J. Sci.* **1983**, *283*, 29–71.
79. Bussolesi, M.; Grieco, G.; Tzamos, E. Olivine-spinel diffusivity patterns in chromitites and dunites from the Finero Phlogopite-Peridotite (Ivrea-Verbanò Zone, Southern Alps): Implications for the thermal history of the massif. *Minerals* **2019**, *9*, 75.
80. Donaldson, C.H. The rates of dissolution of olivine, plagioclase, and quartz in a basalt melt. *Min. Mag.* **1985**, *49*, 683–693.
81. Costa, F.; Dungan, M. Short time scales of magmatic assimilation from diffusion modeling of multiple elements in olivine. *Geology* **2005**, *33*, 837–840.
82. Arculus, R.J.; Delano, J.W. Intrinsic oxygen fugacity measurements: Techniques and results for spinels from upper mantle peridotites and megacryst assemblages. *Geochim. Cosmochim. Acta* **1981**, *45*, 899–913.

Disclaimer/Publisher's Note: The statements, opinions and data contained in all publications are solely those of the individual author(s) and contributor(s) and not of MDPI and/or the editor(s). MDPI and/or the editor(s) disclaim responsibility for any injury to people or property resulting from any ideas, methods, instructions or products referred to in the content.